Université de Montréal

Use of a Novel Peripheral Nerve Conduit to Support Sciatic Nerve Regeneration in an Animal Model

Par

Timothy Lan Chun Yang

Faculté de médecine

Mémoire présenté en vue de l'obtention du grade de maîtrise

en sciences biomédicales, option médecine expérimentale

Juin 2021

Université de Montréal

Programmes de cycles supérieurs en sciences biomédicales, Faculté de médecine

---

Ce mémoire intitulé

Use of a Novel Peripheral Nerve Conduit to Support Sciatic Nerve Regeneration in an Animal Model

Présenté par

Timothy Lan Chun Yang

A été évalué(e) par un jury composé des personnes suivantes

Dre. Dominique Tremblay

Président-rapporteur

Dre. Jenny Catherine Lin

Directrice de recherche

Dre. Svetlana Matei

Membre du jury

Résumé

Introduction : Les conduits nerveux synthétiques représentent une alternative chirurgicale aux autogreffes dans la réparation des traumatismes aux nerfs périphériques. Afin d'améliorer la régénération nerveuse périphérique, plusieurs biomatériels, tels que la multicouche polyélectrolyte de soie (MPE), et modèles ont été étudiés. Dans le cadre de ma maitrise, nos objectifs de recherche sont d'établir si la MPE de soie permet d'améliorer la régénération nerveuse périphérique in vivo et si notre nouveau modèle de conduit (« jelly roll ») peut mener à une meilleure régénération du nerf sciatique chez le rat que le modèle de conduit creux.

Méthodes : Dans cette étude, une technique chirurgicale in vivo de lacération et de réparation du nerf sciatique chez le rat fut utilisé. Cinq conditions expérimentales de conduits (autogreffe, conduit creux avec et sans MPE de soie et « jelly roll » avec et sans MPE de soie) furent implantées (n= 2 rats par condition). Après 4 semaines, les conduits furent récupérés et marqués par immunohistochimie avec le neurofilament et la protéine basique de la myéline (MBP). La performance de chaque conduit fut évaluée par sa capacité à supporter l'excroissance axonale à travers le long du conduit et à travers la largeur de ce dernier à divers endroits.

Résultats : Chaque condition expérimentale a supporté une régénération axonale avec différents degrés de succès. Globalement, l'autogreffe a supporté une plus longue croissance de fibres. De plus, la surface de fibres obtenue était plus large que les autres conditions. Les conduits avec la MPE de soie ont eu une performance similaire à leurs homologues sans soie. De plus, le modèle de conduit creux a mené à une meilleure régénération axonale que le modèle du « jelly roll ».

Conclusion : L'autogreffe demeure le meilleur conduit pour supporter la régénération nerveuse périphérique. Les conduits avec la MPE de soie peuvent supporter une régénération nerveuse similaire aux conduits sans soie tandis que le modèle de « jelly roll » a généré des performances inférieures au modèle de conduit creux.

Mots-clés : régénération nerveuse périphérique, conduit de guidage nerveux, autogreffe nerveuse, multicouche polyélectrolyte de soie, conduit nerveux creux, jelly roll, chirurgie du nerf périphérique, lésions nerveuses périphériques, excroissance axon

Abstract

Background: Synthetic nerve conduits constitute alternative surgical options to autografts in the repair of peripheral nerve injuries. Silk polyelectrolyte multilayer (PEM) as a biomaterial and novel conduit designs have been proposed to improve peripheral nerve regeneration. In my master's project, my objective is to assess whether silk PEM can improve peripheral nerve regeneration *in vivo* and to assess whether our novel conduit design ("jelly roll") can better support rat sciatic nerve regeneration than a hollow conduit design.

Methods: In this study, an *in vivo* rat model of sciatic nerve laceration and repair was used. Five experimental conduit conditions (autograft, hollow conduit with and without silk PEM, and jelly roll with and without silk PEM) were implanted (n=2 rats per condition). After 4 weeks, the conduits were harvested and immuno-stained for neurofilament and myelin basic protein (MBP). Conduit performance was assessed by its ability to support axonal outgrowth throughout the conduit's length and at various locations along its width.

Results: Each condition supported axonal regeneration at varying levels of success. Overall, the autograft group outperformed all other groups by supporting the longest and widest occupying regenerating fibers. Conduits with silk PEM performed similarly to conduits without silk PEM. In addition, the hollow conduit design demonstrated better regenerative outcomes than the jelly roll design.

Conclusion: The autograft remains the superior conduit to support peripheral nerve regeneration. Conduits with silk PEM support nerve regeneration in the same capacity as non silk-coated conduits while the jelly roll design underperformed in comparison to the hollow conduit design.

Keywords : peripheral nerve regeneration, nerve guidance conduit, nerve autograft, silk polyelectrolyte multilayer, hollow nerve conduit, jelly roll, peripheral nerve surgery, peripheral nerve injuries, axonal outgrowth

Table des matières

Liste des tableaux

Liste des figures

Liste des sigles et abréviations

°C: Celsius

° : Degrees (rotation)

mg: Milligram

kg: Kilogram

mL: Milliliter

L : Liter

nm : Nanometer

mm: Millimeter

min : Minute

PEM: Polyelectrolyte multilayer

NaCl: Sodium chloride (referring to a saline solution)

NF: neurofilament

MBP: Myelin Basic Protein

UV: Ultraviolet

NGC: Nerve guide conduit

SC: Schwann cell

NGF: Nerve growth factor

NT-3: neurotrophin-3

GDNF: glial cell-line derived neurotrophic factor

ECM: Extracellular molecules

A: Autograft

HC: Hollow conduit without silk polyelectrolyte multilayer

HS: Hollow conduit with silk polyelectrolyte multilayer

JR: Jelly roll without silk polyelectrolyte multilayer

JS Jelly roll with silk polyelectrolyte multilayer

OCT compound: Optimal cutting temperature compound

PBS: Phosphate-buffered saline

PFA: Paraformaldehyde

hiHS: Heat inactivated horse serum

GFP: Green fluorescent protein

Je souhaite dédier ce mémoire à mes chers parents, Richard et Flora. Je vous remercie de vos encouragements, de votre soutien et de votre amour inconditionnel. Vous êtes ma source d'inspiration, de fierté, d'amour, de soutien, de réconfort et d'énergie qui m'a permis de braver ces deux années de maîtrise. Bien que la route fut longue, ensemble, on peut tout faire.

Remerciements

Dre. Jenny Catherine Lin, pour m'avoir donné l'opportunité de compléter ma maîtrise sous sa supervision et dans son laboratoire. Merci de m'avoir aidé tout au long de mon parcours académique et de m'avoir soutenu dans mes ambitions de carrière.

Dr. Timothy Edward Kennedy, pour m'avoir autorisé à mener mes expériences dans son laboratoire et de m'avoir offert son expertise et son support tout au long de ma maîtrise.

Dr. Christopher J. Barrett, pour m'avoir offert son expertise durant mes expériences et son support à travers mes études.

Anaïs Robert, pour son soutien inconditionnel et son expertise sur les manipulations en laboratoire. Merci de m'avoir aidé durant les nombreuses heures que nous avons passées ensemble afin de faire mes expériences en immunohistochimie.

Victoria Chang, pour ses conseils et sa connaissance de la soie qui furent d'une grande aide lors de mes expériences.

Michel Paquet, pour son soutien sans limites et les nombreuses heures passées ensemble afin de s'assurer de la bonne progression de mon projet. Merci de m'avoir enseigné les techniques chirurgicales et de laboratoire nécessaires pour compléter les diverses expériences dans le cadre de ma maîtrise.

Vincent Weung-Jy Cheung, pour tout son soutien et ses encouragements durant nos 2 ans de maîtrise ensemble. Merci de m'avoir aidé durant les innombrables heures que nous avons passées ensemble que ce soit durant les chirurgies, les expériences en laboratoire, durant nos trajets entre le MNI et le CHUSJ, et même en soirée lors de nos échanges. Je suis très reconnaissant d'avoir eu un partenaire de laboratoire qui m'ait soutenu jusqu'au bout, et dont je considère comme étant devenu mon meilleur ami.

Xindy Yang, pour le soutien qu'elle m'a offert durant les chirurgies que nous avons accomplies ensemble et de son intérêt soutenu.

Le Fonds Apogée et l'Institut TransMedTech, pour avoir financièrement soutenu mon projet de recherche.

Ma famille et mon entourage, pour leur soutien et leurs conseils durant ma maîtrise.

1. Chapter 1 - Introduction

1.1 Clinical issues in the treatment of peripheral nerve injuries

The peripheral nervous system has an intrinsic regenerative capacity after suffering from injury (Faroni, Mobasseri, Kingham, & Reid, 2015). Axons can spontaneously regenerate over relatively short distances, typically less than 5mm (Jiang, Lim, Mao, & Chew, 2010). Peripheral nerve injuries can be caused by trauma or medical disorders, which, in turn, can cause significant morbidity and permanent disability (Ciaramitaro et al., 2010; Noble, Munro, Prasad, & Midha, 1998; Taylor, Braza, Rice, & Dillingham, 2008). Most traumatic cases of nerve injuries occur in the upper limbs (Kouyoumdjian, 2006). Upper limb function is essential, not only for gross and fine motor activities, but also in our everyday activities (self-care, self-expression, work) and how we interact with the world around us (Raichle, 2008). Therefore, when patients suffer from a severe case of peripheral nerve injury, it can have a devastating impact on their quality of life. Chronic symptoms from these injuries can include sensory and motor defects which can result in partial or complete paralysis of the affected limb or the development of neuropathic pain (Rivera, Glebus, & Cho, 2014; Siemionow & Brzezicki, 2009).

In addition, the presence of physical gaps between nerve ends is very common as neuromas must be excised before surgical intervention and this can represent a major hurdle for surgical reconstruction and functional recovery (Poppler et al., 2018; Wolvetang et al., 2019). Wallerian degeneration also remains one of the major biological barriers to rapid and complete nerve regeneration and recovery. It is agreed in the literature that axonal regeneration occurs at 1 mm/day within two- or three-days post-injury. Over large distances, such as a nerve gap of over 20 cm, functional recovery is severely affected and is usually incomplete (Bittner, Schallert, & Peduzzi, 2000; Grinsell & Keating, 2014). As a result, the primary goal of nerve repair is the reinnervation of downstream targets by guiding the regenerating sensory, motor, and autonomic axons into the distal nerve with minimal loss (Kurze, 1964).

In order to address the biological limitations of peripheral nerve regeneration, the clinical gold standard for repairing physical gaps in peripheral nerves remains the autologous autograft

(Hoben et al., 2018). The most commonly used autologous nerve for nerve graft is the sural nerve (Andersen et al., 2015; Spinner, Shin, & Bishop, 2015). Autografts fulfill the criteria for an ideal nerve conduit as they facilitate axon regeneration to the distal nerve and end-organ targets by providing a permissive and stimulating scaffold with Schwann cell basal laminae, neurotrophic factors and adhesion molecules (Hoben et al., 2018; Siemionow & Brzezicki, 2009). Therefore, autografts are the preferred option to bridge nerve gaps longer than 3 cm, for proximal injuries and critical nerves (Pfister et al., 2011).

However, the use of the autograft comes with several major shortcomings as well. The main disadvantage is the sacrificing of a functioning nerve (sensory nerve like the sural nerve) in order to serve as the donor nerve. This creates sensory loss, skin numbness and scarring at the donor site and can cause painful neuromas to form (Gerth, Tashiro, & Thaller, 2015; Marchesi et al., 2007; Moore, Ray, Chenard, Tung, & Mackinnon, 2009). Furthermore, the option to utilize the autograft as a surgical intervention is restricted by the lack of available and expendable donor nerves and potential donor site complications (FF, Nicolai, & Meek, 2006; Hallgren, Björkman, Chemnitz, & Dahlin, 2013; Martins et al., 2012). This is particularly problematic when an initial autograft has failed and a repeat nerve graft is needed, thus resulting in a second surgical site, which only increases patient morbidity (Chen, Yu, & Strickland, 2007; Pulley et al., 2016). Additionally, a clinical rule of thumb is that there is a 50% loss of axon regeneration that occurs at each coaptation site. As a result, for nerve repair involving one coaptation site, around 50% of the original axons will successfully regenerate through the repair site, while for nerve grafts, which include two coaptation sites, only 25% of axons are expected to regenerate through the graft (Grinsell, 2014). Finally, there is an unavoidable nerve size and fascicle mismatch with use of autografts and scarring at the repair site can lead to poor regeneration (Grinsell, 2014). Longer distances to the motor or sensory target will incur additional axonal loss due to chronic axotomy and muscle fibrosis (Grinsell, 2014). However, despite these shortcomings, the nerve autograft still provides the most complete regenerative environment for regenerating axons that is currently available (Hoben, 2018).

In order to address the issues that can be caused with use of nerve autografts, some surgeons have turned to nerve entubulation as an alternative method of treatment. This concept uses a

"nerve tube" that acts as a physical guide for regenerating nerves and reduces unwanted interactions between regenerating axons and myofibroblasts at the injury site to diminish scarring (Jiang, 2010). Therefore, the focus has shifted towards the development of biological and synthetic nerve guide conduits (NGCs) (Jiang, 2010). These are needed in order to alleviate the need for secondary injury at the harvesting site while fulfilling a role to guide regenerating axons from the proximal end to the distal segment (Jiang, 2010; Grinsell, 2014).

1.1.1 Biological nerve conduits

The first kind of biological NGCs include hollow vein and arterial conduits, as well as soft tissues such as muscle and tendon grafts (Grinsell & Keating, 2014; Konofaos & Ver Halen, 2013). Vein conduits have shown to produce similar results to sural nerve digital grafts, but their use is reserved for small, less important nerves over short nerve gaps (less than 3 cm) (Chiu & Strauch, 1990; Riccio, Marchesini, Pugliese, & De Francesco, 2019).

A second kind of biological NGCs are human cadaveric nerve allografts (Moore, 2009). Unlike autografts, the use of allografts is not restricted by donor supply limitation or donor site morbidity (Moore, 2009). However. due to the fact that cadaveric allografts contain donor Schwann cells that may display non compatible major histocompatibility complexes which can incite a T-cell response in the recipients, patients must be immunosuppressed for up to two years until the donor nerve graft has been repopulated with host Schwann cells (Griffin, Hogan, Chhabra, & Deal, 2013). As a result, nerve allotransplantation can incur significant costs and their use is complicated which is why it should be reserved for unique patients with irreparable peripheral nerve injuries (Moore, 2009).

More recently, a technique for decellularizing nerve allografts has been commercialized in order to avoid drawbacks of patient immunosuppression (Karabekmez, Duymaz, & Moran, 2009). These commercially available allografts (AxoGen©) are more advantageous than hollow nerve conduits because their internal structure provides endoneurial tubes, basal lamina and laminin which can facilitate axonal regeneration (Karabekmez, 2009). However, the use of these allografts is still limited to small sensory nerves (digital nerves) for nerve gaps smaller than 3 cm, and this type of

graft is not considered a replacement for autologous autografts in motor nerves, in proximal nerve injuries and in gaps longer than 3 cm (Cho et al., 2012).

1.1.2 Synthetic nerve conduits

Other groups have looked at producing synthetic NGCs in order to ease mass-production and to allow custom designs (Jiang, 2010). Materials to produce these conduits often utilize purified extracellular matrix (ECM) molecules such as collagen (type I, III, or IV) or laminin because they possess cell-adhesive or signaling domains which may represent a more biologically appropriate microenvironment for nerve regeneration (Jiang, 2010). In addition, animal studies have shown that collagen conduits demonstrated similar efficacy as autograft, although, clinical studies are still lacking (Grinsell, 2014; Griffin, 2013). These types of conduits are currently commercialized as hollow conduits (mostly biodegradable polymer or collagen-based hollow tubes) but fail to match the levels of nerve regeneration that autografts attain (Pabari, Lloyd-Hughes, Seifalian, & Mosahebi, 2014). As a result, the use of synthetic NGCs is limited to repairing short nerve gap distances (<2cm) and often result in poorer functional recovery than obtained with autografts (Pabari, 2014).

Synthetic polymers can also be specifically tailored to match different desired properties (degradation time or compositions) which may represent an advantage over NGCs made from biological materials (Jiang, 2010). However, so far, synthetic polymers have been shown to support limited nerve regeneration when used as empty NGCs to treat nerve injuries above a critical nerve gap (~3 cm in humans and 1.5 cm in rats) (Schlosshauer, Dreesmann, Schaller, & Sinis, 2006). Often, functional recovery is also poor. Instead, more promising nerve regeneration has occurred when synthetic NGCs (polyglycolic acid (PGA), polylactide-co-caprolactone (PLCL) and collagen) were used to bridge nerve gaps over shorter distances (Jiang, 2010; Schlosshauer, 2006).

1.1.3 Commercially available synthetic nerve conduits

Although current commercially available synthetic NGCs may be made out of various biomaterials with different properties, they all share the same design of being hollow conduits (NeuraGen®, Integra LifeSciences©, Princeton, New Jersey; Neuroflex®, Collagen Matrix©, Oakland, New

Jersey; Neurolac ®, Polyganics ©, Groningen, Netherlands; Neurotube®, Synovis Micro Companies Alliance©, Birmingham, Alabama; Salutunnel®, Salumedica©, Atlanta, Georgia). Furthermore, despite company claims about the performance of these conduits supporting regeneration of up to 3 cm, many of them do not actually support nerve regeneration well when used in clinical settings at these distances. Their use for nerve gaps above 3 cm is even more limited, and they are not commonly used in repair of mixed nerves (Gerth, 2015). Therefore, a better NGC is still needed, and many groups continue to experiment with different designs and materials.

1.2 New generation of nerve conduits and designs

Since peripheral nerve regeneration through hollow NGCs are not optimal, considerable efforts have now been invested in designing a new generation of nerve conduits by exploring different avenues of innovation (Jiang, 2010). Additional research has started looking at the necessary factors in order to promote regeneration across long lesion gaps. As such, considerations for conduit designs now also include biochemical molecule signaling, neurotrophic factors, usage and delivery of Schwann cells, presence of physical scaffolds, conduit topography, and other promising biocompatible materials like silk (Deumens et al., 2010; Muheremu & Ao, 2015).

1.2.1 Hybrids and biochemical molecule signaling

Many of the new designs involve combining some of the previously mentioned considerations in order to form structures that resembles naturally occurring ones or to reconstitute bio-environments favorable for nerve regeneration. For example, in order to create a structure like the bands of Büngner, which occur when Schwann cells (SCs) form longitudinally-oriented cables during the nerve regeneration process, NGCs can be engineered in order to contain specific forms and shapes of internal scaffolds in order to imbed the adequate density of Schwann cells to stimulate nerve regeneration (Muheremu, 2015). In addition, designing new kinds of polymers as the building materials for NGCs addresses several of the drawbacks posed by previous generations of NGCs, such as loss of mechanical stability after surgical implantation, release of acidic degradation products and the lack of fine control of degradation rate (Jiang, 2010). As such, developing materials that can serve the dual purpose of both acting as a polymeric conduit and

as a drug delivery vehicle for cells or drugs to enhance axon regeneration or function recovery constitute more interesting options for clinicians and researchers (Jiang, 2010).

1.2.2 Neurotrophic factors

Neurotrophic factors play key roles in controlling the survival, proliferation, migration and differentiation of several nerve cell types which are crucial during nerve regeneration. Some novel NGC designs have sought to prolong the availability of neurotrophic factors in targeted tissues by controlling the timing of their release (Jiang, 2010). Nerve growth factor (NGF), neurotrophin-3 (NT-3), glial cell-line derived neurotrophic factor (GDNF) and fibroblast growth factors have been used by different groups. As a result, being able to encapsulate these various types of neurotrophic factors within the lumen of the NGC and time their release into the lumen are particularly interesting. By configuring the release timing of factors as the conduit undergoes degradation, it may better mimic the natural biochemical signaling that occurs during nerve repair which may then promote better neuronal survival, growth and proliferation for improved nerve regeneration (Jiang, 2010; Deumens, 2010).

1.2.3 Schwann cells

The delivery of Schwann cells (SCs) into NGCs may enhance nerve regeneration as they play a crucial role in supporting axonal migration and regrowth following nerve injuries in the PNS (Schlosshauer, 2003; de Ruiter, 2009). SCs naturally secrete neurotrophic factors (like NGF) (de Ruiter, Malessy, Yaszemski, Windebank, & Spinner, 2009), promote the formation of blood vessels and potentially determine the embedding of connective tissues (Schlosshauer, 2003). Furthermore, SCs produce extracellular matrix molecules (ECM) such as laminin and collagen, and express neural cell adhesion molecules and receptors which can guide the growth of axons (Lietz, Dreesmann, Hoss, Oberhoffner, & Schlosshauer, 2006; Muheremu & Ao, 2015). SCs can also help bridge longer nerve gaps by forming longitudinally-oriented cables (bands of Büngner) for axons to regenerate along whereas otherwise, following implantation of a hollow NGC, the fibrin matrix may not form inside the conduit from the proximal and distal nerve ends if the gap is too long (de Ruiter, 2009). Nonetheless, adequate structural support is required at the injury site in order to

ensure the survival of SCs inside the lumen of NGCs. Therefore, some groups have used hydrogels to serve as the supporting substrate in which SCs are delivered into the lumen (Jiang, 2010).

1.2.4 Presence of physical scaffolds

In order to complement the regeneration process, some groups have introduced luminal contact guidance structures into NGCs in order to enhance SC alignment. After nerve injuries, the bands of Büngner normally form prior to the axonal regeneration step. As such, if SCs fail to migrate across the nerve gap in hollow conduits, poor regeneration may result, especially in cases of a large gap defect (Jiang, 2010). Therefore, the presence of contact guidance, such as intraluminal silk or collagen fibers or other material providing a surface of contact, may ensure the successful migration of SCs across the lesion gap and the promotion of early SC alignment may speed the healing process (Jiang, 2010; Muheremu, 2015).

1.2.5 Topography

In retrospect, it was noted that the lumen of hollow conduits quickly becomes filled with loose fibrin matrix after implantation, which probably forms as part of a blood clot under the activation of endogenous tissue repair mechanisms in the PNS. This matrix supports the migration of perineurial cells from the severed nerve ends, and is then followed by infiltration of endothelial cells, fibroblasts, SCs and, ultimately, by regenerating axons (Deumens, 2010). By virtue of adopting a hollow conduit as the initial design to demonstrate the stereotypic sequence of events during peripheral nerve regeneration, researchers have pointed to the importance of the internal structure of the NGC because they may affect its physical properties, such as permeability and flexibility, and may affect the total cross-sectional area available for regenerating axons (de Ruiter, 2009). Further analyses have determined that the physical and chemical properties of intra-luminal contents and the substrate microstructure, may influence cell shape, growth of regenerating axons and the accuracy of regeneration across the conduit (de Ruiter, 2009; Deumens, 2010). In response, several groups have sought to create microstructures and scaffolds inside of NGCs in order to mimic the longitudinally orientated anatomy of peripheral nerves. Orientation of biomaterials and scaffolds have been achieved by using polymer extrusion or polymer alignment by magnetic fields, injection molding, phase separation and micropatterning

(Dubey, Letourneau, & Tranquillo, 2001; Hadlock, Sundback, Hunter, Cheney, & Vacanti, 2000; Yoshii & Oka, 2001). Moreover, the topography of the fibers or grooves inside the NGC can have serious effects on the guidance and orientation of regenerating cells and their process even on the scale of microns (Jiang, 2010).

1.2.6 Shortcomings of new generation conduits and designs

Despite the development of these promising conduit designs and the inclusion of more features that may support peripheral nerve regeneration, most of these strategies are still being investigated *in vitro* and *in vivo*. Furthermore, none of these experimental models are currently available on the market except for biodegradable hollow conduits. In addition to the lack of clarity on which strategy is best, many of the attempted molecular, neurotrophic or topographical additions are not feasible commercially. For example, the inclusion of Schwann cells via a delivery system into the lumen of the nerve conduit would be very difficult to accomplish during surgical operations and mass production of SC cells for their inclusion in commercially available NGCs is even less feasible. Proposed methods to avoid immune rejection include taking SCs from the umbilical stem cells or other tissues such as autologous adipose tissues which only further complicates the task at hand (Muheremu, 2015).

1.3 Why use silk in conduits?

Collagen and synthetic polyester–based materials have had rather lackluster success in their ability to bridge large nerve gaps in current clinical settings (Magaz et al., 2018). On the other hand, silk as a biomaterial has become a prominent choice in the field of nerve tissue engineering. Research has been conducted on silk fibroin originating from silkworms (Bombyx mori) and spider sources (Magaz et al., 2018, Deumens, 2010). Fibroin is the core structural protein of silk and it has been shown to have good biocompatibility with PNS cells in vitro (Yang et al., 2007).

1.3.1 Uses of silk

Silk is also commonly utilized in clinical settings as sutures during soft tissue repair and it is FDA-approved as an implantable biomaterial (Magaz, 2018). Its rise in popularity is due to its many physicochemical, mechanical, and biological properties which make it an ideal substrate for nerve repair. (Magaz, 2018). First, it can stimulate oxygen and water permeability, which are essential for nutrient and water-soluble metabolite transport (Magaz, 2018). It can form fibrous scaffolds which may support cell attachment and the proliferation of neurons and SCs without causing any adverse effects (Magaz, 2018; Jiang, 2010). Furthermore, it possesses high tensile strength and toughness while also providing the suitable flexibility necessary to prevent the collapse of the conduit (Magaz, 2018; Deumens, 2010; (Vollrath, Barth, Basedow, Engström, & List, 2002). These are crucial in order to avoid any secondary operations or long-term adverse effects of the implant (Magaz, 2018). In addition, silk is a biocompatible material as it only triggers relatively low levels of inflammatory responses (Magaz, 2018). Most importantly, silk fibroin can easily be tuned to the desired chemical, mechanical and biological properties by selecting a specific manufacturing source (silkworm or spider), by blending the silk with various other polymers or by giving it specific morphologies such as gels, membranes, nanofibers and foam-like forms (Magaz, 2018). In addition, it is possible to create synthetic recombinant silk fibroin in order to reduce batch-to-batch variations, which enables their mass production, and partial gene sequences may be tuned to the silk specific functionalities (Magaz, 2018).

Silk may also be arranged in such a way that it can incorporate and deliver neurotrophic growth factors, proteins and even cells into the NGC which may address many of the concerns

encountered by the previously mentioned strategies to promote peripheral nerve regeneration (Magaz et al., 2018; Deumens, 2010). For example, silk fibroin conduits containing NGF and GDNF, and lined with silk fibroin nanofiber have been shown to support good axon growth and glial cell migration in DRG explants in vitro (Deumens, 2010).

In a study conducted by Yang et al. hollow conduits, manufactured from silk fibroin were lined with longitudinally orientated fibroin filaments in order to promote axon regeneration across a 1cm nerve gap in an adult rat sciatic nerve (Yang, 2007). Over a 6-month period, axon regeneration and functional recovery were assessed by electrophysiological measurement of compound muscle action potentials (CMAP) and a retrograde tracing technique using fluorogold and immunohistochemistry (Yang, 2007). Not only did the silk NGC lead to no systemic or local signs of inflammation, but there were no statistically significant differences between the CMAP amplitudes following the implantation of the silk fibroin conduit or nerve autograft. In addition, no differences were detected in the number of retrogradely labeled DRG sensory neurons or ventral horn motor neurons between the silk fibroin conduit or the autograft (Yang (a), 2007). It was concluded that silk fibroin, as a biomaterial, can support substantial axonal regeneration and tissue repair over relatively small defects of 1cm (Yang, 2007).

Primary mammalian neural cells such as neurons and oligodendrocytes are particularly difficult to maintain and grow in cell cultures (Landry et al., 2019). Therefore, an appropriate supportive substrate must be used in *in vitro* environments in order to closely mimic *in vivo* conditions. The standard “state-of-the-art” culture substrate consists of a single layer of poly-D-lysine (PDL). However, this layer is fragile and can be damaged by drying or UV light, degraded by proteolysis, and cannot be stored for long periods of time due to its instability (Landry et al., 2019). The alternative isomeric form, poly-L-lysine (PLL), is therefore widely used as a standard surface to culture neural cells as it provides a non-specific attachment factor for cells (Landry, 2019). However, these substrates are relatively expensive to produce, are prone to degradation, and thus must be made immediately prior to their use.

1.3.2 Silk-based polyelectrolyte multilayers (PEMs)

Polyelectrolyte multilayers (PEMs) constitute a promising material for the design of an improved substrate for neural cell culture. PEMs are films fabricated from polyelectrolytes which are water-soluble polymers. They are assembled through a layer-by-layer method (Sailer, 2012; Landry, 2019). Landry et al. established that silk-based PEMs are significantly better than PDL or synthetic polyelectrolytes at covering the surface area of neuronal cell culture material, and these PEMs act as bio-camouflage on a non-compatible surface by causing the coated surface to be relatively more soft and wet, mimicking a composition similar to that of an ECM (Landry, 2019). In order to obtain successful biocamouflage, silk-based PEMs had better desired chemical functionality and water content which translated into a superior and effective substrate coating for neural cell culture (Sailer, Lai Wing Sun, Mermut, Kennedy, & Barrett, 2012). Furthermore, using silk fibroin is relatively inexpensive compared to PDL/PLL, can easily be assembled into a simple PEM coating of SF-PL (silk fibroin from B. mori co-polymerized with PLL and polyacrylic acid (P(AA-co-DR1A)) and can be assembled weeks in advance because of its relative shelf-stability (Landry, 2019).

1.4 Developing the prototype conduit

Our novel design for a nerve conduit incorporates several of the most promising experimental features based on previous studies. This prototype conduit reunites the structural properties of collagen-based conduits while including the benefits of the silk PEM in supporting neural cell growth and adding intraluminal physical properties that have been identified as important in the literature. The chosen design resembles a "jelly roll", consisting of layers of collagen layered with or without silk PEM and fibrin glue.

We combined collagen sheets layered with SF-PL PEM and used fibrin glue to roll the sheets into the prototype NGC. In order to provide more intraluminal substrate for axonal regeneration, the collagen sheet layered with SF-PL was rolled onto itself while the fibrin glue provided the necessary material to maintain the shape of the conduit, thus resembling a "jelly roll". Fibrin glue was selected because it is a biodegradable biopolymer and mimics the last step of blood coagulation which results in a fibrin clot (Li, Meng, Liu, & Lee, 2015). As a result, the fibrin clot can be used as an adhesive to bind the conduit to native nerve tissue in order to prevent leakage of fluid and, in turn, would decrease the number of needed sutures at each coaptation site. In addition, fibrin glue is regularly used as a bioadhesive in surgical settings for hemostasis, wound closure, and especially as a sealant at coaptation sites during peripheral nerve repair (Childe et al., 2018; Jackson, 2001; Langer, Schildhauer, Dudda, Sauber, & Spindler, 2015; Li et al., 2015).

1.5 Research objectives

In my master's work, the main objectives are to 1) test the jelly roll design in peripheral nerve regeneration in the rat sciatic nerve model and to 2) test the ability of silk PEM based conduits in supporting axonal outgrowth when utilized *in vivo*.

2. Chapter 2 – Methods

2.1 Experimental design

In this study, 10 male Lewis rats were used (n = 10) to test the capacity of various experimental conditions of nerve guide conduits to support axonal outgrowth from a peripheral nerve. Using an established *in vivo* rat model of sciatic nerve laceration and repair (Beaumont, Cloutier, Atlan, Rouleau, & Beaumont, 2009), the rats were divided into 5 experimental conditions of nerve guide conduits: autograft, hollow conduit with silk PEM, hollow conduit without silk PEM, jelly roll with silk PEM and jelly roll without silk PEM (n=2). For each group, the conduit was implanted and then harvested 4 weeks later for each experimental condition. In this study, the experimental conditions will be denoted as follows:

- Autograft condition: A1 or A2 in reference to the rat subject
- Hollow conduit without silk PEM condition: HC1 or HC2 in reference to the rat subject
- Hollow conduit with silk PEM condition: HS1 or HS2 in reference to the rat subject
- Jelly roll without silk PEM condition: JR1 or JR2 in reference to the rat subject
- Jelly roll with silk PEM condition: JS1 or JS2 in reference to the rat subject

These 5 experimental conditions were chosen for this pilot project in order to assess, either individually or combined, the effectiveness of silk PEM as a substrate to support peripheral nerve regeneration in a *in vivo* model and to assess a novel luminal conduit structure (referred to as "jelly roll") for its ability to increase the available surface area for regenerating axons.

Since commercially available collagen nerve conduits are very expensive, and their design could easily be replicated (NeuraGen®), we decided to create our own collagen conduit equivalent out of collagen sheet. The sheet would then be sutured in order to give it a tube-like shape. Collagen was chosen as the base material for all experimental conditions because it is one of the materials of choice for currently available conduits on the market. Due to its biocompatible properties, its commercial availability and due to its low cost, different variations of conduits can be produced. Furthermore, collagen is a material that can be easily paired with silk PEM.

The rat model was chosen for its reduced cost and anatomical similarity to human nerves which makes it a reliable model to study axonal regeneration (Menorca, Fussell, & Elfar, 2013; Swett, Wikholm, Blanks, Swett, & Conley, 1986). The rats were obtained from Charles River Laboratories. The animals were housed at the CR-Sainte-Justine animal facility in a temperature-controlled environment, maintained on a 12h/12h light/dark cycle and provided with feed and water ad libitum. All experimental protocols were approved by the Animal Ethics Committee of the Sainte-Justine Hospital research center.

2.2 Autograft protocol

The autograft condition aimed to serve as a control condition to represent the surgical gold standard of the autograft used in human patients. To simulate the process, a 15mm segment of the sciatic nerve was excised, thus leaving behind a proximal and distal nerve stump. The proximal nerve stump refers to the end of the injured neuron still attached to the neuron cell body in the spinal cord which can undergo regeneration while the distal nerve stump refers to the end of the injured neuron that is still attached to the end of the axon and will degenerate over time. The severed nerve segment is then reoriented the other way around (180°) before being sutured back onto the nerve. As axons throughout the severed nerve section and the distal nerve stump undergo Wallerian degeneration over the first week after injury, the traumatic damage to the sciatic nerve will induce a state of axonal regrowth and innervation (Menorca et al., 2013). The progressive breakdown of the nerve will make way for newly regenerating axons (Menorca et al., 2013). The inversion of the autograft was done to replicate the clinical conditions of nerve grafting and prevent the loss of axons through branch points.

2.3 Silk PEM preparation

The silk PEM was constructed as described by Landry et al (2019), wherein the collagen sheet was dipped and coated with the silk PEM solution (Figure 1).

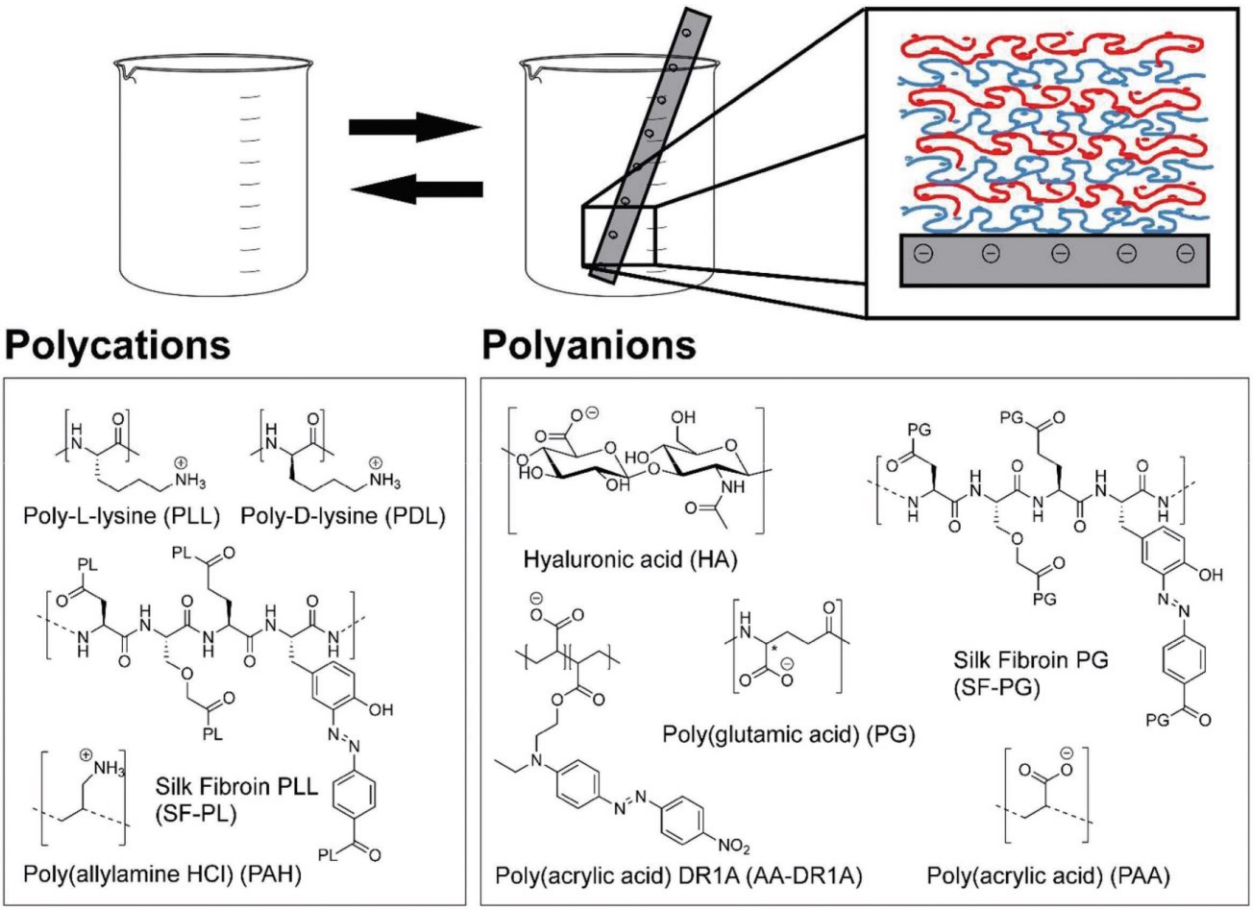

Figure 1. – Construction of the silk PEM as described by Landry et al. (2019). Top: Schematic depicting layer-by-layer assembly of PEM films, beginning with a negatively charged substrate (collagen) being dipped in a polycation solution. Bottom: Illustration of biologically relevant polycationic and polyanionic polymers. For this study, the chosen polycation is silk Fibroin PLL while the chosen polyanion is Poly(acrylic acid) DR1A (AA-DR1A). Figure obtained with authorization from publisher John Wiley and Sons.

2.4 Hollow conduit with and without silk PEM preparation protocol

A 15 x 20 mm piece of collagen sheet was cut out and sterilized under UV light in a fume hood. The collagen sheet was then rolled with two microsurgery forceps until the extremities overlapped in order to form a 1.5 to 2mm diameter wide conduit of 15mm in length. The conduit shape was then secured by using a running suture (nylon 6-0 Ethicon^{TM}) along the length of the

conduit. The hollow conduit was then sterilized under UV light in a fume hood. The conduit was placed in a sterilized petri dish and kept at 4°C until the moment of implantation.

A 15 x 20 mm piece of collagen sheet layered with silk PEM was prepared from the samples obtained from our collaborators from the Barrett lab at the Department of Chemistry of McGill University. The collagen sheet was then prepared to form a 15mm-long hollow conduit with silk PEM under the same conditions as the hollow conduit without silk PEM and stored at 4°C until ready for implantation (Figure 2).

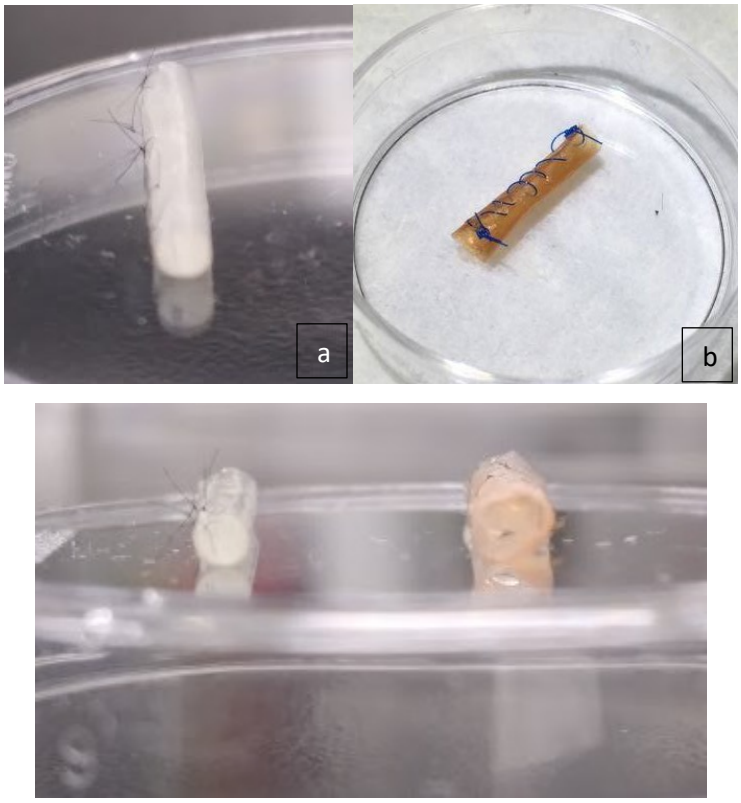

Figure 2. – Hollow conduit without silk PEM (a) and Hollow conduit with silk PEM (b). Both conduits were made from 15 x 20 mm pieces of collagen sheet (a) or collagen coated with silk PEM (b).

2.5 Fibrin glue preparation protocol and jelly roll conduit with and without silk PEM preparation protocol

20mg of fibrinogen lyophilized powder from bovine plasma (≥ 60 NIH units/mg protein (biuret)) (Sigma Aldrich) were diluted in 1mL of 0.9% NaCl saline solution in order to prepare a fibrinogen

solution at a 20mg/mL concentration in a 5mL Eppendorf tube. 10mg of thrombin from bovine plasma (Type I-S, 65-85% protein (≥75% of protein is clottable) (Sigma-Aldrich) were diluted in 10mL of 0.9% NaCl saline solution in order to prepare a thrombin solution at a 1mg/mL concentration in a 20mL tube. Both solutions were then kept at 4°C until ready to be used for making the jelly roll.

The jelly roll with and without silk PEM were prepared by dispensing 0.9mL of thrombin solution [1mg/ml] and 1mL of fibrinogen solution [20mg/ml] using a 30G needle onto a 15 x 20 mm piece of collagen or silk PEM coated collagen. After 3 minutes, the thrombin and the fibrinogen coagulated to form a fibrin glue. Once coagulation is achieved, the collagen is then tightly rolled onto itself in order to form a 15mm-long prototype conduit with a diameter of about 15 to 20 mm (Figure 3). The conduits were then stored at 4°C overnight.

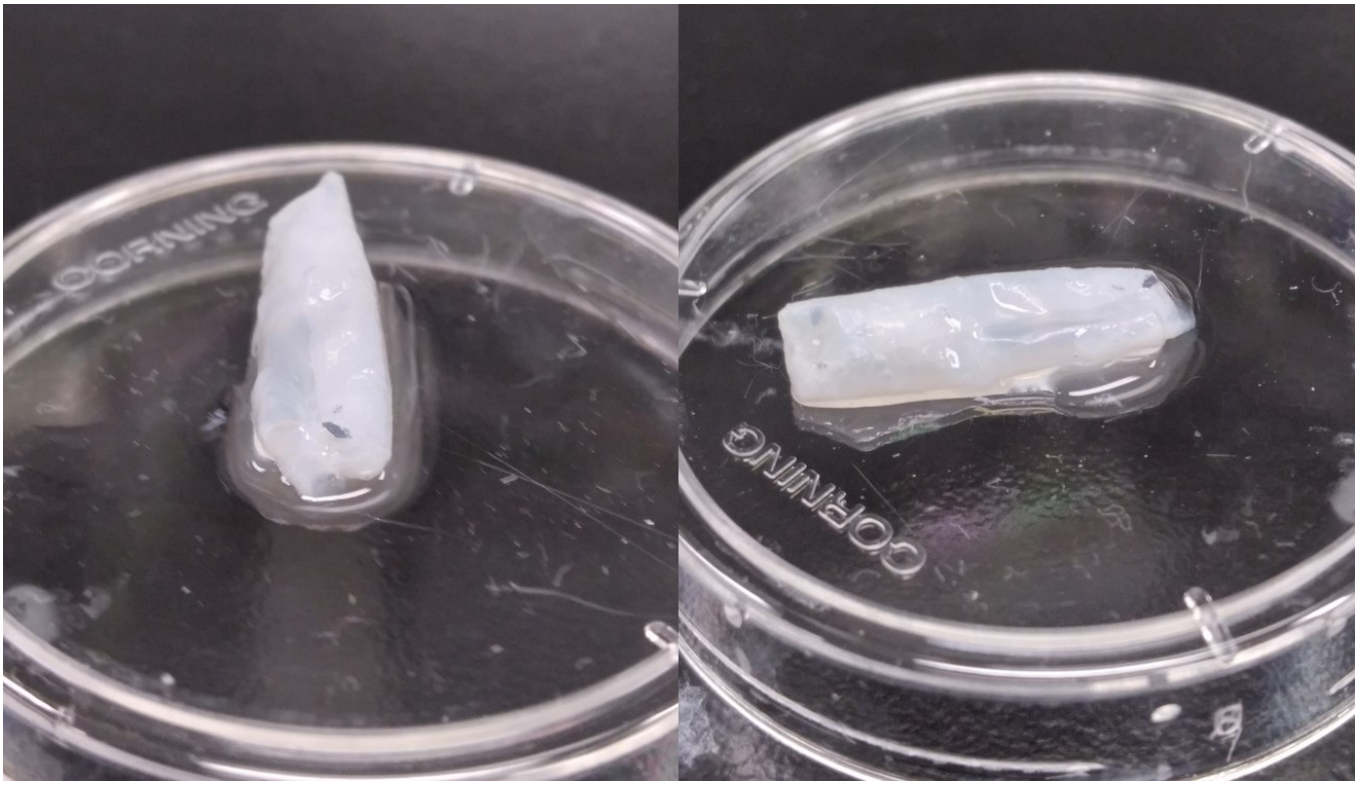

Figure 3. – Jelly roll without silk PEM. Fibrin glue is applied onto a 15 x 20 mm piece of collagen and then tightly rolled onto itself once the glue has coagulated.

2.6 Nerve Conduit Implantation Surgery

Rats were anesthetized with Isoflurane (3-5% in 1.5L/min O2) in an induction chamber and placed on a ventral position on a heated mat with their snouts placed into a tube which dispensed Isoflurane (1-2.5% in 0.4-0.8L/min O_2). The left leg was shaved and was wiped with 70% ethanol and Proviodine in preparation for surgery. Sub-cutaneous administration of Buprenorphine (0.05-0.1 mg/kg) was then performed to reduce post-operative pain. An incision of 3-4cm wide was made along the femur and a pair of scissors were used to loosen fascia from muscle groups. The biceps femoris, tensor fasciae latae and parts of the gluteus maximus muscle groups were separated using forceps and scissors in order to access the sciatic nerve.

Using microsurgical tools, the connective tissues and membranes were separated from the sciatic nerve (Figure 4 and Figure 5). Once cleared, 15 mm of the nerve was excised and removed to make way for the nerve conduit or, in the autograft condition, the nerve was reoriented backwards then sutured back. A nerve conduit was placed in the nerve gap and attached with two sutures of nylon 8-0 (Ethicon^{TM}) at each extremity where the nerve stump and conduit meet, called the coaptation site. At the proximal coaptation site, the proximal nerve stump is sutured to one end of the conduit (will be referred to as proximal end of the conduit) while the distal nerve stump is sutured to the other end of the conduit (will be referred to as distal end of the conduit). The surgical site was regularly hydrated with 0.9% saline in order to prevent tissues from drying. After checking that bleeding was stopped, the skin was closed with a non-resorbable 4-0 suture. Five mg/kg Enroflaxacin (Baytril) and 1.0 ml of 0.9% saline were administered subcutaneously post-surgery. Post-surgical follow-up occurred after 24 hours in order to administer Buprenorphine (0.1 mg/kg) subcutaneously, and additional visual follow-up throughout the following days were performed to ensure the rats did not exhibit any signs of distress.

Figure 4. – Surgical and microsurgical instruments used during the implantation and harvest surgeries. Surgical tools were used to access the sciatic nerve while microsurgical instruments were used for implantation.

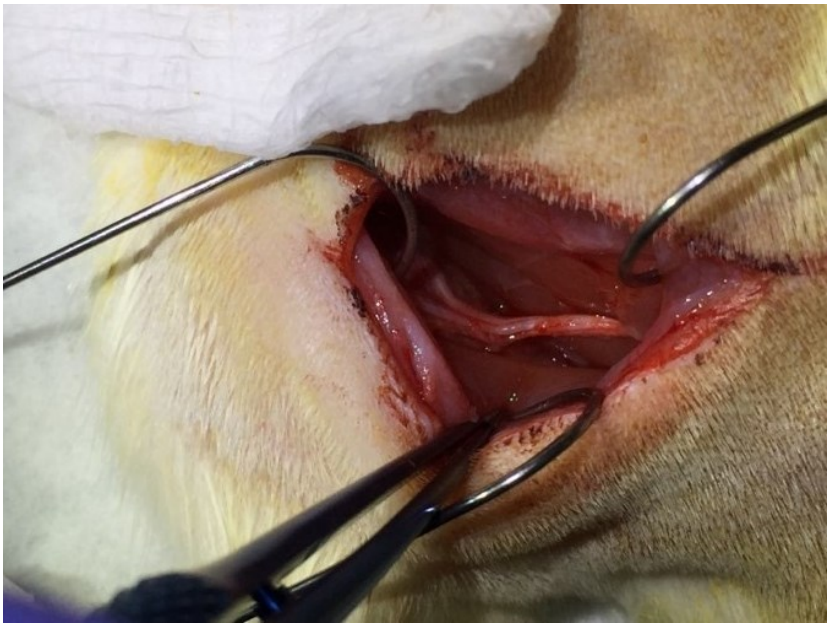

Figure 5. – Accessing the sciatic nerve conduit during implantation surgery. With the help of surgical tools, the sciatic nerve can be exposed and accessible after the surrounding connective tissue has been removed.

2.7 Harvest surgeries

Harvest surgeries occurred 4 weeks following the initial surgical implantation of the nerve conduit condition or the autograft. Utilizing the same surgical techniques and methods, the nerve conduits were separated from connective tissues and the nerve conduits were retrieved along with 1-2mm of sciatic nerve on both extremities (proximal and distal nerve stumps) (Figure 6). At the end of the harvest surgeries, the rats were sacrificed according to our animal facility's protocols.

Figure 6. – Dimensions of harvested nerve conduits. Example of a harvested nerve conduit along with 1-2mm of proximal and distal nerve stump.

2.8 Fixing and 30% sucrose cryoprotection

All harvested nerve conduits were fixed in paraformaldehyde (PFA) (4%) for 1 hour after being extracted from the rats. The specimens were then washed three times and cryoprotected in 30% sucrose phosphate-buffered saline (PBS) overnight at 4°C. The following day, the specimens were

embedded in OCT compound in cryomolds at -20°C with the use of dry ice. The frozen samples were then kept at -20°C until ready for sectioning.

2.9 OCT and cryostat sectioning

All specimen samples were sliced longitudinally at 16µm thickness using a Cryostat Thermo CryoStar NX50 at -16 °C (Figure 7). The samples were then placed on microscope slides and were stored at -20 °C.

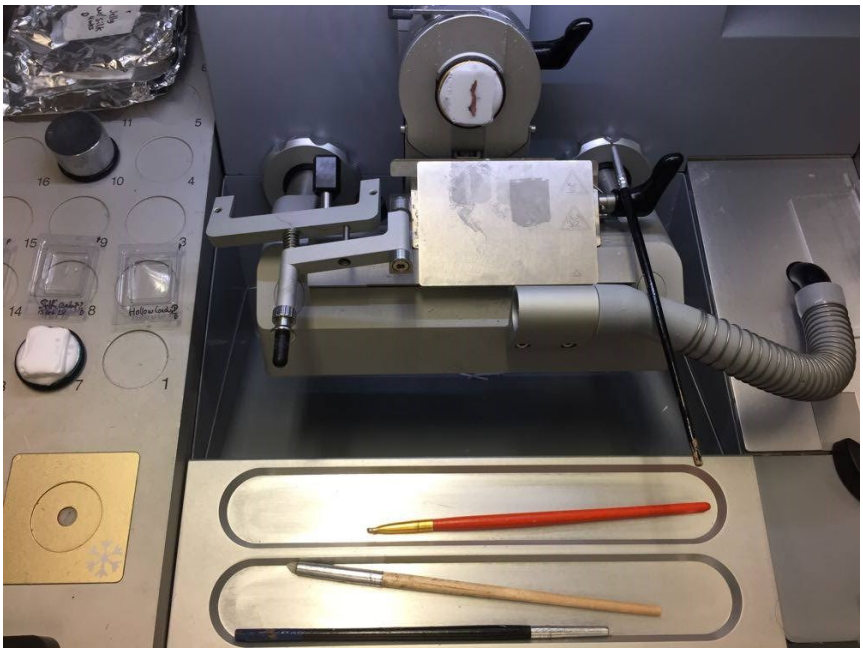

Figure 7. – Cryostat Thermo CryoStar NX50. This cryostat model was used to section longitudinal slices of specimen samples onto microscope slides. Slice thickness was 16µm.

2.10 Immunohistochemistry (IHC) staining protocol

Specimen samples were washed twice in PBS then blocked for 1 hour with 3% heat inactivated horse serum (hiHS) and 0.25% triton x-100. Afterwards, primary antibodies rabbit Neurofilament light chain (1:1000 ratio) (Thermo-Fisher) and chicken Myelin Basic Protein (MBP) (1:5000) (Thermo-Fisher) were added to the specimen samples and incubated at 4◦C overnight. The following day, the samples were washed three times in a buffer solution of PBS with 1% hiHS and 0.1% triton x-100 before secondary antibodies (Alexa Fluor 488 goat anti-rabbit and 647 goat anti-chicken) (Thermo-Fisher) were applied onto the samples at a 1:1000 ratio with PBS with 1% hiHS

and left to incubate at room temperature for 2 hours. After incubation, the samples were washed three times in PBS before mounting with Fluoro-gel mounting media (Electron Microscopy Sciences). The positive control used for the experiment was healthy rat sciatic nerve tissue while negative controls included a 1cm x 1cm sheet of both collagen and collagen coated with silk PEM. The slides were left to dry overnight before imaging.

2.11 Microscope imaging

Image acquisition was performed using a Leica DMI-8 inverted wide-field microscope (Figure 8). A 10X objective with a 1X magnification was used for the imaging of the entire specimen. The image resolution was set to 0.65 x 0.65 um per pixel. Two fluorescent cube filters were chosen to visualize and image the peak fluorophore emission wavelengths of neurofilament and MBP. The GFP filter was chosen because its excitation filter transmits light from 450nm to 490nm, corresponding to a green emission color, and the Y5 excitation filter transmits light from 590nm to 650nm, corresponding to a far-red emission color (Figure 9). The settings for the inverted wide-field microscope were kept constant for the entirety of the image acquisition process of all specimens.

Figure 8. – Leica DMi-8 wide-field microscope. A 10X objective with a 1X magnification was used for the imaging of the specimen for each experimental condition.

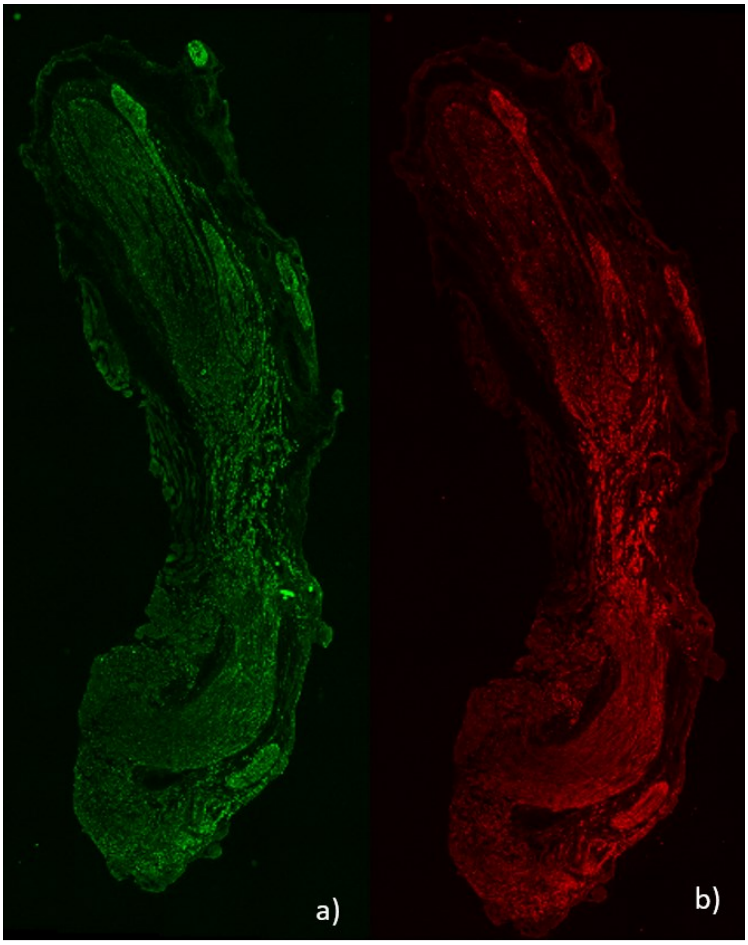

Figure 9. – Excitation wavelengths used for microscope imaging. The GFP excitation filter transmits light from 450nm to 490nm (green emission color) (a), and the Y5 excitation filter transmits light from 590nm to 650nm (far-red emission color)(b). In this example, one specimen from Autograft 1 is shown.

2.12 Data analysis

2.12.1Average distance of regenerated axon through each experimental condition

Utilizing the Leica microscope software (LAS X), the total length of the conduit and the furthest regenerating axons (neurofilament and MBP) starting from the proximal coaptation site for every tissue sample were measured (Figure 10). The length of neurofilament and MBP fibers regenerating through the conduit was measured and recorded on an Excel sheet for each tissue sample in all five experimental conditions. The length measurements for each experimental conduit condition was then averaged to provide the average length achieved by regenerating axons (neurofilament and MBP) in the conduit (Table 1). 10 tissue samples were analyzed for each nerve conduit in all five experimental conditions, with the exception of JR1 where only 5 tissue samples were analyzed.

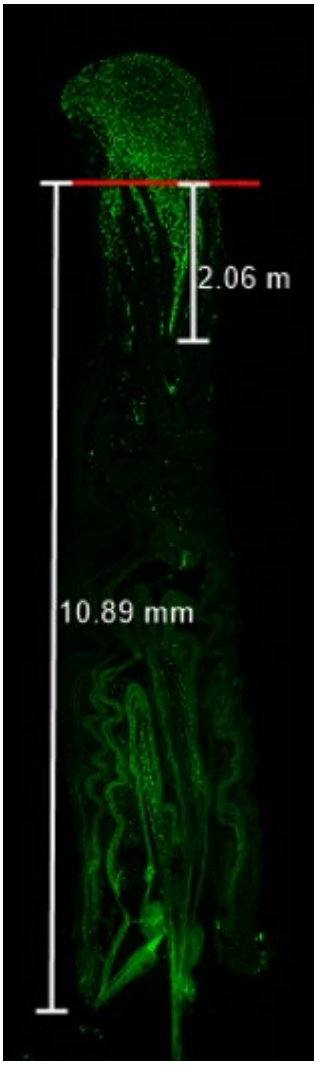

Figure 10. – Autograft and conduit length measurement method. The total length of the conduit and the furthest regenerating axons starting from the proximal coaptation site for every tissue sample were measured. The red lines indicate the proximal coaptation site at the top of the image and the distal coaptation site at the bottom of the image.

2.12.2Average width of regenerated axons through each experimental condition

Utilising the LAS X software, width of the conduit and width of regenerating axons were measured at the proximal end, at the mid-conduit and at the distal end, when possible. The proximal end refers to the location where the conduit begins at the proximal coaptation site while the distal end refers to the point where the conduit ends at the distal coaptation site. The mid-conduit point

refers to the area of the conduit that is found halfway from the proximal end and the distal end (Figure 11).

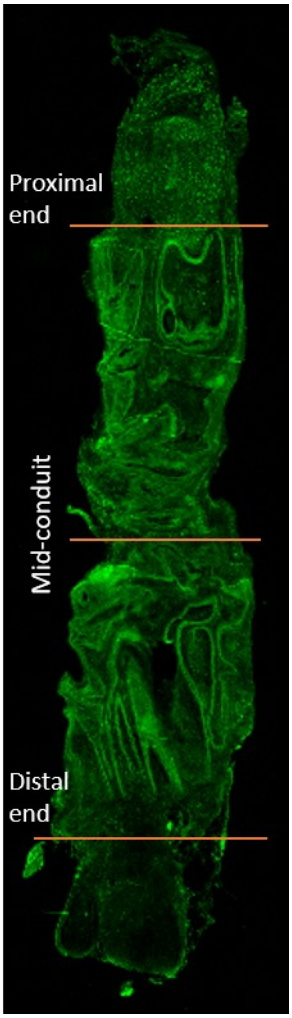

Figure 11. – Identification of the proximal end, mid-conduit and distal end. The proximal end references the proximal coaptation site while the distal end references the distal coaptation site. The mid-conduit point refers to the area that is found halfway from the proximal end and the distal end.

The width of fibers stained with neurofilament and MBP across the conduit at various locations was measured and recorded on an Excel sheet for each tissue sample in all five experimental conditions. In order to not artificially increase the width measurements of regenerating fibers due to the compartments created by the lumen of the conduit, only the immediate width of regenerating bundle of fibers was measured (Figure 12).

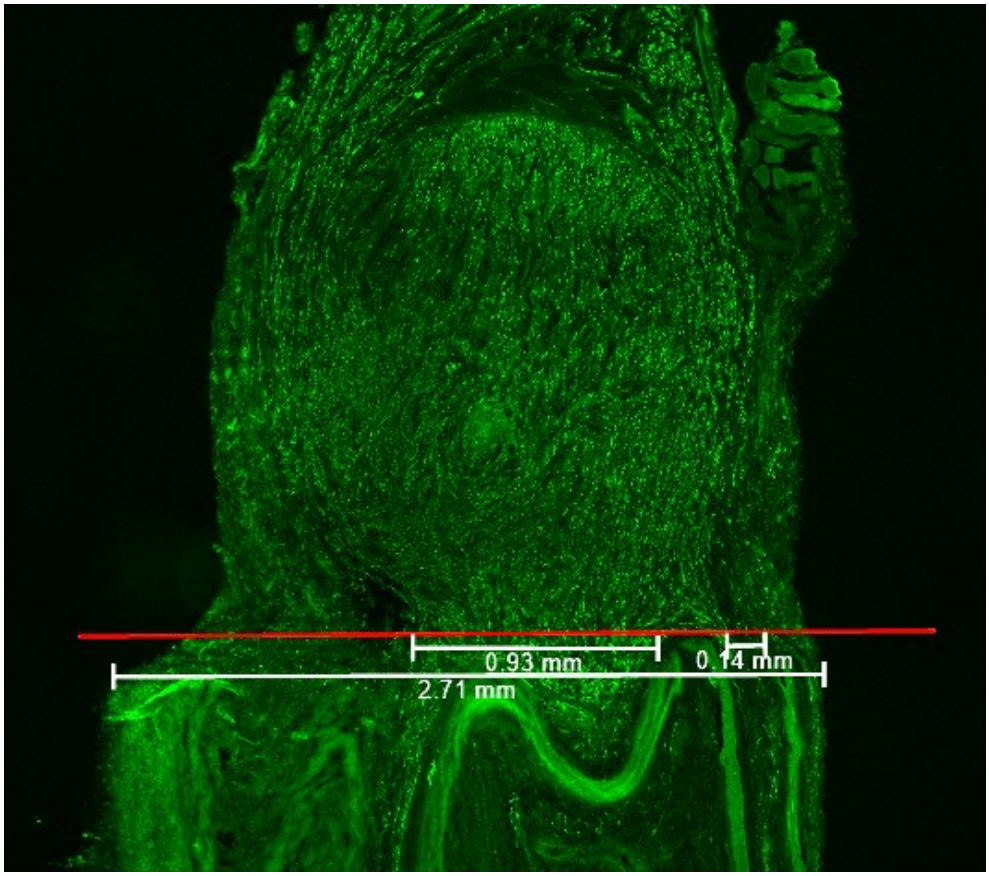

Figure 12. – Method of measurement of the width of regenerating bundles of fibers and measurement of the width of the conduit. Only the width of each regenerating bundles of fibers was measured in order to not artificially inflate the width measurement. In this example, the width of regenerating bundles of fiber stained by neurofilament is 1.07cm (0.93cm + 0.14cm)while the width of the conduit is 2.71cm. The red line indicates the proximal coaptation site.

The width measurements for each nerve conduit was then averaged to provide the average width occupied by regenerating axons (neurofilament and MBP) at each measurement location in the conduit (Table 1). 10 tissue samples were analyzed for each nerve conduit in all five experimental conditions, with the exception of JR1 where only 5 tissue samples were analyzed.

2.12.3 Percentage of length and width covered by regenerating axons for neurofilament and MBP

To contrast how much distance in length regenerating axons (neurofilament and MBP) have gone through the conduit, the average length for neurofilament or MBP were divided by the total length of the nerve conduit (average neurofilament or MBP length in mm / average length of conduit). This ratio provides a percentage which refers to the nerve conduit's performance in supporting regenerating axons along its length. This ratio calculation was also applied for all average width measurements in relationship to the conduit's average width at various locations (proximal end, mid-conduit and distal end, when possible) to provide in percentage the nerve conduit's performance in supporting regenerating axons across its width at various locations (Table 2). Finally, an overall performance of the experimental condition group as a whole was obtained by combining the individual performance of each nerve conduit assigned to that group (e.g. performance of A1 + A2 = performance of autograft group) (Table 3).

3. Chapter 3 – Results

3.1 Image analysis

After 4 weeks, tissue specimens of all five experimental conditions and all rat subjects were processed, cryo-sliced, immunostained and then imaged by the Leica DMI-8 inverted wide-field microscope. Using the LAS X software, dimensions of the conduit such as length and width were measured along with the length and width of regenerating axons as immunostained by neurofilament and MBP on every single tissue sample slide. The data was compiled on Excel in order to produce the average length and width of regenerating axons stained by neurofilament and MBP at various locations (proximal end, mid-conduit and distal end, when possible) and the percentage at which axons had regenerated into the conduit in comparison to the conduit's total length and width at various locations. 10 tissue samples were imaged and analyzed per rat subject per experimental condition with the exception of the jelly roll without silk PEM (JR1) where only 5 tissue samples were imaged and analyzed.

3.2 Immunohistochemistry and control experiments

Neurofilament constitutes a major part of the cytoskeleton of axons. Immunohistochemistry with specific antibodies to neurofilaments has been used in experimental studies on axonal regeneration in order to make these structures visible (Meller, Bellander, Schmidt-Kastner, & Ingvar, 1993). Myelin Basic Protein (MBP) is an useful antibody because when used in immunohistochemistry, it allows for the easy identification of myelination of neuroanatomic sites while requiring low power from a microscope (Bodhireddy, Lyman, Rashbaum, & Weidenheim, 1994). As such, neurofilament and MBP can help identify sites where regeneration of axons is occurring while also discriminating from structures that are part of the conduit.

Positive control consisted of a healthy rat sciatic nerve (Figure 13). Negative controls consisted of a 1cm x 1cm collagen sheet and a 1cm x 1cm collagen sheet coated with silk PEM. Both positive and negative controls were immunostained with neurofilament and MBP by IHC (Figure 13).

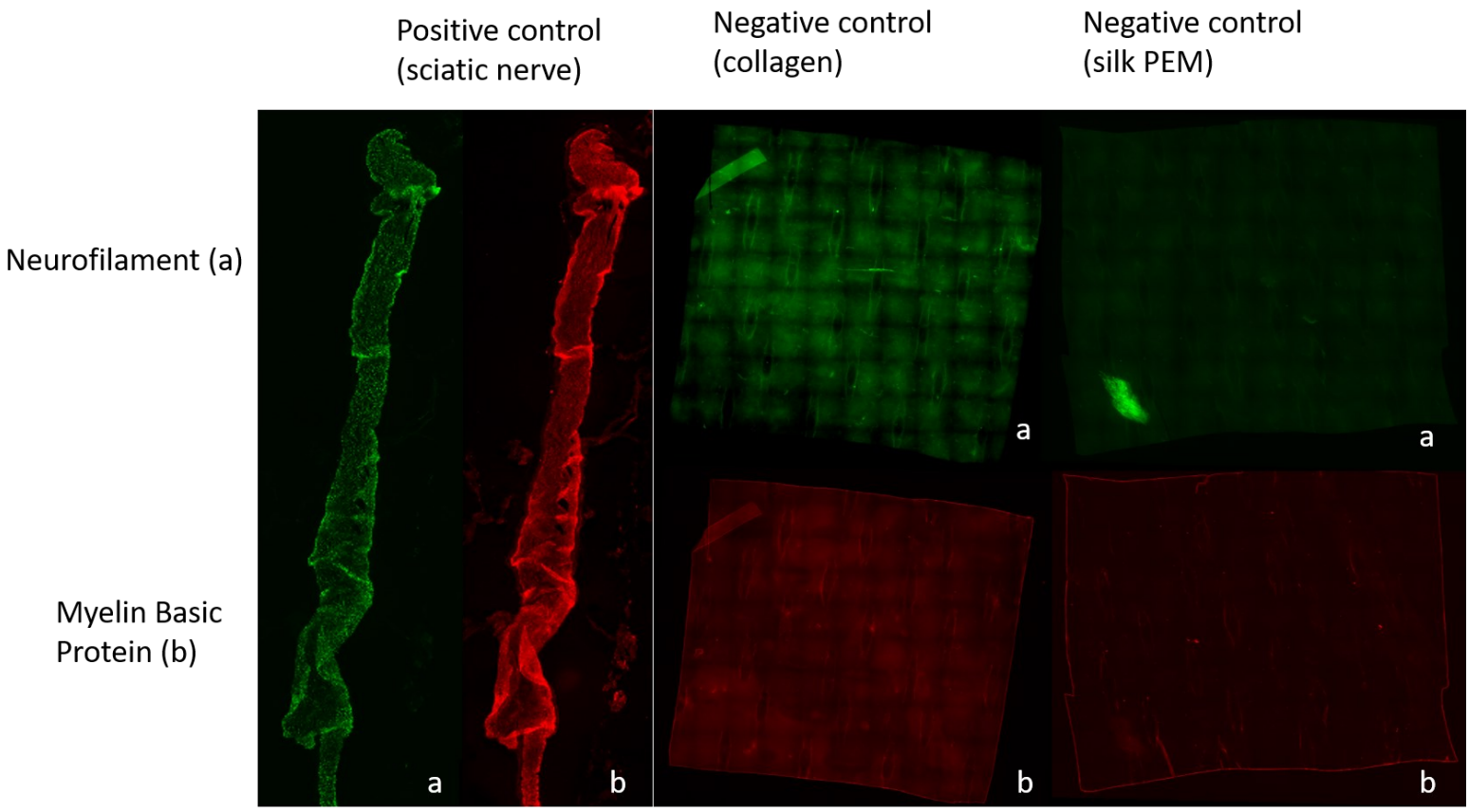

Figure 13. – Positive and negative controls. Positive control consisting of a healthy rat sciatic nerve immunostained with neurofilament (a) and MBP (b). Negative controls consisting of a 1cm x 1cm collagen sheet and a 1cm x 1cm collagen sheet coated with silk PEM. Both sheets were immunostained with neurofilament (a) and MBP (b).

3.3 Autograft experiment

In the autograft implantation experiment, the two autografts (auto 1 and auto 2) measured 7.5mm and 12mm long, respectively, while their width was on average 1.70mm and 1.51mm, respectively, after 4 weeks. In A1, 90.3% of regenerating neurofilament covered on average 6.77mm in length with an average neurofilament width coverage of 1mm (74.9%) at the proximal end, 0.86mm (72.1%) in the middle of the conduit and 1.96mm (76.2%) at the distal end. MBP average coverage reached 6.27mm (83.5%) while its average width coverage was 0.73mm (54.5%) at the proximal end, 0.64mm (53.7%) at the mid-conduit and 1.68mm (65.2%) at the distal end.

In A2, neurofilament regeneration reached on average 11.51mm in length (95.9%) while it covered, on average, 0.86mm (77.2%) at the proximal end, 1.40mm (81.9%) at the mid-conduit, 1.18mm (69.0%) at the distal end. As for MBP, it has covered on average 10.76mm (89.7%) in length while its width average coverage was 0.66mm (59.2%) at the proximal end, 1.12mm (89.7%) at mid-conduit and 0.64mm (37.3%) at the distal end.

3.4 Hollow conduit without silk PEM experiment

In the hollow conduit without silk PEM experimental condition, at time of harvest after 4 weeks of implantation, the two conduits were 11.51mm and 12.89mm in length, respectively. The conduits had an average width of 2.15mm in HC1 (1.87mm at the proximal end and 2.43mm between the proximal end and mid-conduit) and 1.42mm in HC2 (0.99mm at the proximal end and 1.84mm between the proximal end and mid-conduit). Neither neurofilament nor MBP were detected at the mid-conduit and distal end of the conduit.

In HC1, neurofilament reached on average 5.09mm (44.3%) in length and reached, on average, 1.41mm (75.2%) in width at the proximal end. On the other hand, MBP reached on average 3.68mm (32.0%) in length and covered, on average, 1.22mm (65.3%) in width at the proximal end.

In HC2, neurofilament reached 2.69mm (20.7%) on average in length and reached, on average, 0.69mm (67.1%) in width at the proximal end. Myelin regeneration via MBP staining measured, on average, 2.15mm (16.7%) in length and covered, on average, 0.60mm (60.6%) in width at the proximal end.

3.5 Hollow conduit with silk experiment

After being harvested 4 weeks post-surgical implantation, in the hollow conduit with silk PEM experimental condition, the two conduits measured 13.82mm and 13.68mm in length, respectively. The conduits had an average width of 2.17mm in HS1 (1.74mm at the proximal end and 2.59mm between the proximal end and mid-conduit) and 2.14mm in HS2 (1.93mm at the

proximal end and 2.34mm between the proximal end and mid-conduit). Neither neurofilament nor were detected at the mid-conduit or the distal end of either hollow conduits with silk PEM.

In HS1, the neurofilament fibers reached a length of 6.75mm (48.8%) on average and covered, on average, a width of 1.13mm (64.8%) at the proximal end of the conduit. Myelination of axons (MBP) reached an average length of 5.40mm (39.%) in HS1 while covering an average of 1.12mm (64.2%) at the proximal end.

As for HS2, neurofilament penetrated the conduit at an average length of 2.29mm (16.8%) while occupying an average width of 0.77mm (39.8%) at the proximal end. As for myelin basic protein, fibers were shown to have grown to an average length of 1.18mm (8.6%) and to an average width of 0.76mm (39.3%) at the proximal end.

3.6 Jelly roll without silk PEM experiment

At 4 weeks post-implantation, jelly roll without silk PEM conduits were retrieved and measured. The two conduits' length averaged 11.02mm and 10.67mm for JR1 and JR2, respectively. In addition, the average width was measured to be 2.77mm in JR1 (2.76mm at the proximal end) and 2.74mm in JR2 (2.43mm at the proximal end). For both conduits, no neurofilament and MBP were detected at the mid-conduit and distal end points.

JR1 neurofilament fibers were shown to have regenerated to an average of 2.12mm in length which represents about 19.2% of the conduit's total length. As for its width coverage, neurofilament occupied, on average, 0.93mm at the proximal end which represents 33.6% of the total width of the conduit. As for MBP, the staining revealed that myelin has grown up to 1.47mm in length on average, thus, representing 13.4% growth of myelin fibers into the conduit. The width of MBP was measured to be, on average, 0.69mm (25.0%) at the proximal end.

In JR2, neurofilament reached an average length of 2.11mm (19.7%) while achieving an average width of 1.72mm (70.8%) at the proximal. When measuring MBP, the average length of regenerating myelin down the conduit was, on average, up to 1.60mm (15.0%). The total width covered by MBP was around 1.39mm (57.1%) at the proximal end.

3.7 Jelly roll with silk PEM experiment

After being harvested 4 weeks after initial surgical implantation, jelly roll with silk PEM conduits, JS1 and JS2, were measured for their average length and width. JS1 measured 10.74mm in length and 2.62mm in width (2.31mm at the proximal end) . On the other hand, JS2 measured 12.61mm in length and 1.71mm in width (1.52mm at the proximal end). Neurofilament and MBP were not observed at the mid-conduit and distal end points.

In JS1, neurofilament fibers reached an average length of 2.18mm (20.3%) and covered an average width of 1.37mm (59.4%) at the conduit's proximal end. As for MBP, it reached a length of 1.47mm (13.6%) on average and an average width of 1.18mm (51.1%) at the proximal end.

In JS2, neurofilament was found to extend into the conduit up to a length of 1.40mm (11.1%) and occupied a width of 0.98mm (64.3%) at the proximal end. Myelinated fibers as detected by MBP revealed that it grew up to 0.94mm (7.5%) inside the conduit. Its average width at the proximal end extended to 0.78mm (51.1%).

Conduit name	Avg. length (mm)	Avg. width (mm)	Avg. neuro length (mm)	Avg. MBP length (mm)	Avg. neuro width (mid-conduit) (mm)	Avg. MBP width (mid-conduit) (mm)	Avg. neuro width (proximal end) (mm)	Avg. MBP width (proximal end) (mm)	Avg. neuro width (distal end) (mm)	Avg. MBP width (distal end) (mm)
A1	7.5	1.7	6.77	6.27	0.86	0.64	1.00	0.73	1.96	1.68
A2	12	1.51	11.51	10.76	1.40	1.12	0.86	0.66	1.18	0.64
HC1	11.51	2.15	5.09	3.68	-	-	1.41	1.22	-	-
HC2	12.89	1.42	2.67	2.15	-	-	0.67	0.60	-	-
HS1	13.82	2.21	6.84	5.35	-	-	1.11	1.11	-	-
HS2	13.68	2.11	2.28	1.25	-	-	0.79	0.74	-	-
JR1	11.02	2.77	2.12	1.47	-	-	0.93	0.69	-	-
JR2	10.67	2.74	2.11	1.60	-	-	1.72	1.39	-	-
JS1	10.74	2.62	2.18	1.47	-	-	1.37	1.18	-	-
JS2	12.61	1.71	1.40	0.94	-	-	0.98	0.78	-	-

Tableau 1. – Average length and width of regenerating axons (neurofilament and MBP) of each nerve conduit for all experimental conditions. A= Autograft condition, HC= Hollow conduit without

silk PEM condition, HS) Hollow conduit with silk PEM condition, JR= Jelly roll without silk PEM condition, JS= Jelly roll with silk PEM. 1 and 2 denote the rat subject assigned to the experimental condition. Measurements in mm. Neuro= neurofilament, MBP= Myelin Basic Protein.

3.8 Comparison between experimental conditions

3.8.1 Performance of the autograft condition

Among the experimental conditions, autograft 2 was the most efficient conduit at supporting neurofilament regeneration with 95.9% growth throughout the conduit while also achieving an MBP regeneration of 89.7% in length inside the conduit. In addition, A2 also achieved the best regeneration of neurofilament and MBP across the width of the conduit at the proximal end (77.2% for neurofilament) and mid-conduit (81.9% for neurofilament, 65.7% for MBP). However, it was outperformed by autograft 1 (A1) at the distal end point with a higher width of axon regeneration (76.2% vs. 69.0% for neurofilament and 65.2% vs. 37.3% for MBP) (Table 2). Autograft 1 also achieved a similar performance with 90.3% of neurofilament growing through the conduit and 83.5% of MBP repopulating the conduit (Table 2).

Conduit name	Percentage of length covered by neurofilament	Percentage of length covered by MBP	Percentage of width covered by neurofilament (mid-conduit)	Percentage of width covered by MBP (mid-conduit)	Percentage of width covered by neurofilament (proximal)	Percentage of width covered by MBP (proximal)	Percentage of width covered by neurofilament (distal)	Percentage of width covered by MBP (distal)
A1	90.3%	83.5%	72.1%	53.7%	74.9%	54.5%	76.2%	65.2%
A2	95.9%	89.7%	81.9%	65.7%	77.2%	59.2%	69.0%	37.3%
HC1	44.3%	32.0%	-	-	75.2%	65.3%	-	-
HC2	20.7%	16.7%	-	-	67.1%	60.6%	-	-
HS1	49.5%	38.7%	-	-	63.2%	63.1%	-	-
HS2	16.7%	9.1%	-	-	41.7%	39.3%	-	-
JR1	19.2%	13.4%	-	-	33.6%	25.0%	-	-
JR2	19.7%	15.0%	-	-	70.8%	57.1%	-	-
JS1	20.3%	13.6%	-	-	59.4%	51.1%	-	-
JS2	11.1%	7.5%	-	-	64.3%	51.1%	-	-

Tableau 2. – Individual nerve conduit length and width performance in supporting regenerating axons for neurofilament and MBP (%).Performance of all other experimental conditions. The average length/width for neurofilament or MBP was divided by the total length of the nerve conduit/by the conduit's average width at various locations. This ratio provides a percentage to assess the performance of the conduit to support axonal regeneration in length or in width. A= Autograft condition, HC= Hollow conduit without silk PEM condition, HS) Hollow conduit with silk PEM condition, JR= Jelly roll without silk PEM condition, JS= Jelly roll with silk PEM. 1 and 2 denote the rat subject assigned to the experimental condition. Measurements in mm. Neuro= neurofilament, MBP= Myelin Basic Protein.

3.8.2 Performance of all other experimental conditions

All other experimental conditions achieved a length regeneration of under 50% for both neurofilament and MBP. Of those conditions, hollow conduit with silk PEM 1 (HS1) performed the best with 49.5% of the conduit seeing neurofilament regeneration and 38.7% of MBP throughout the conduit. HC1 came in second amongst the non-autograft conduits, as it supported 44.3% of neurofilament and 32.0% of MBP in length. The rest of the other conduits had a length

performance of under 21% with JS2 being the worst with 11.1% and 7.5% for neurofilament and MBP, respectively. Furthermore, HC1 and HS1 length performance was better than both the jelly roll conduits whether they had silk PEM or not. However, HC2 and HS2 performed similarly in length with the jelly roll conditions with the exception of JS2 which did the worst out of all the conduits. Every experimental condition, with the exception of JR1 and HS2, achieved above 50% coverage across the conduit at the proximal end for both neurofilament and MBP. However, all conditions failed to cover more than 35% of the width of the conduit when looking at regenerating axons between the proximal end and mid-conduit region. In addition, all conduits failed to support any regeneration up to and past the mid-conduit (Table 2) (Figure 14 and 15). Furthermore, inner walls of certain experimental conduits were observed to be caved in on themselves or were not straight.

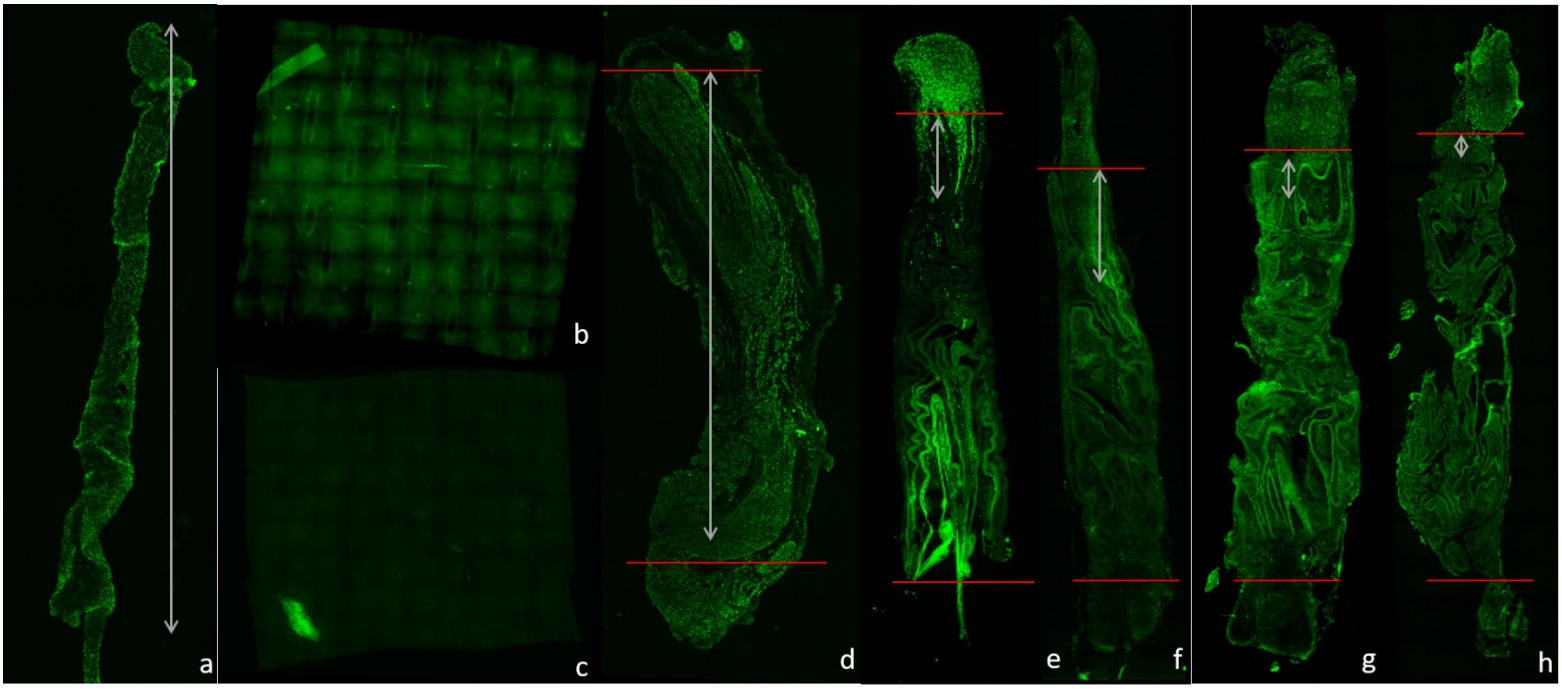

Figure 14. – Overall representation of regeneration along the length of each experimental condition using neurofilament immunostaining. Red lines at the top of the image indicate the proximal coaptation site while the red lines at the bottom of the image indicate the distal coaptation site. Gray arrow bars indicate the area where axonal regeneration was observed. a) Positive control (healthy sciatic nerve), b) negative control (collagen sheet), c) negative control

(collagen coated with silk PEM), d) autograft, e) hollow conduit, f) hollow silk conduit, g) jelly roll, h) jelly roll with silk PEM.

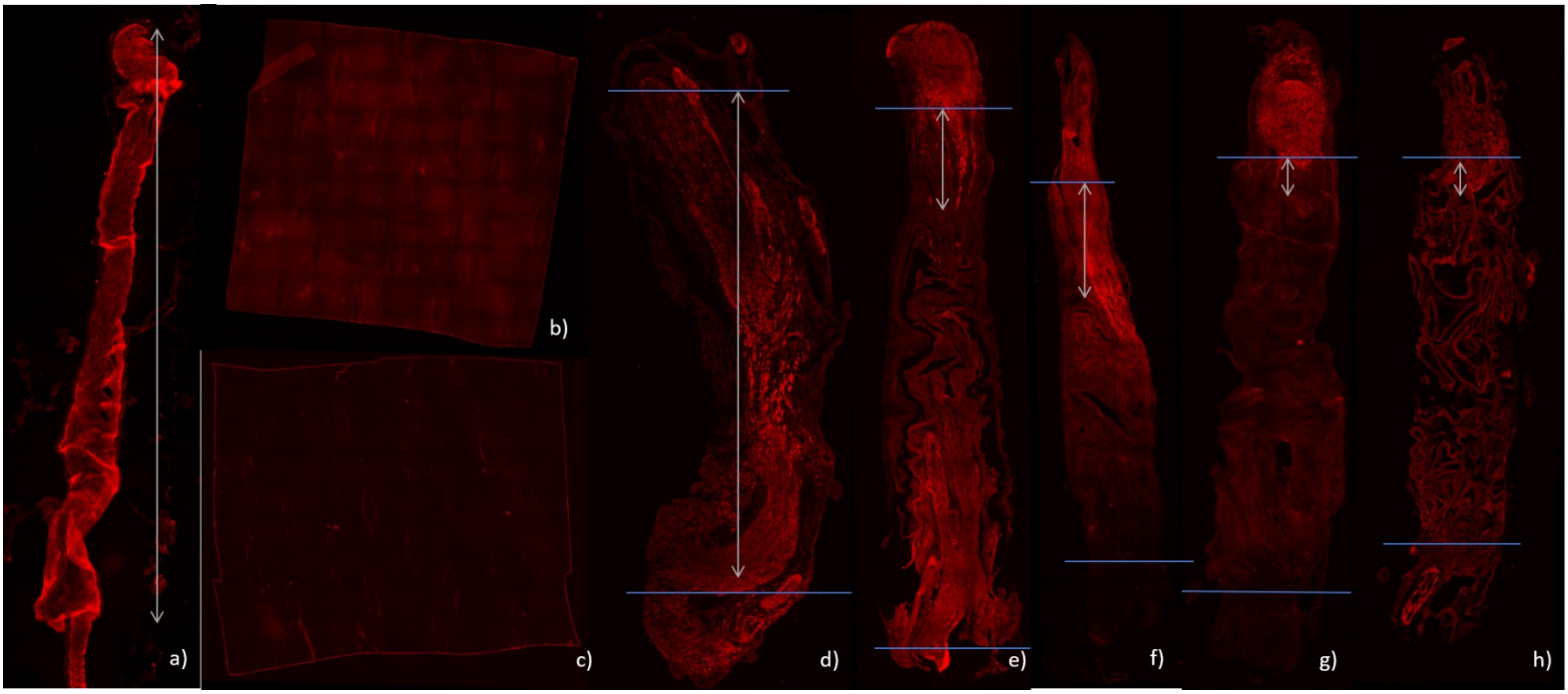

Figure 15. – Overall representation of regeneration along the length of each experimental condition using MBP immunostaining. Blue lines at the top of the image indicate the proximal coaptation site while the blue lines at the bottom of the image indicate the distal coaptation site. Gray arrow bars indicate the area where axonal regeneration was observed. a) Positive control (healthy sciatic nerve), b) negative control (collagen sheet), c) negative control (collagen coated with silk PEM), d) autograft, e) hollow conduit, f) hollow silk conduit, g) jelly roll, h) jelly roll with silk PEM.

3.8.3 Overall group performance

When grouped according to their experimental conditions, the autograft group outperformed every other condition by supporting an overall axon regeneration length of 93.7% and 87.3% throughout the conduit for neurofilament and MBP, respectively. In addition, the autograft group was also the best condition to support axon regeneration across its width with a 75.7% coverage for neurofilament and a 57.2% coverage for MBP.

In comparison, the other experimental conditions did not support neurofilament regeneration above 35% and myelination (MBP) above 25% of the conduit's length. When looking at overall group performance, both hollow conduit groups had a better length performance for neurofilament and MBP than both the jelly roll groups. On the other hand, these four groups had similar width performances whether it be at the proximal end. In addition, when comparing silk PEM groups (HS and JS) to their non-silk PEM counterparts (HC and JR), the silk groups perform similarly to their non-silk homologues in both length and width.

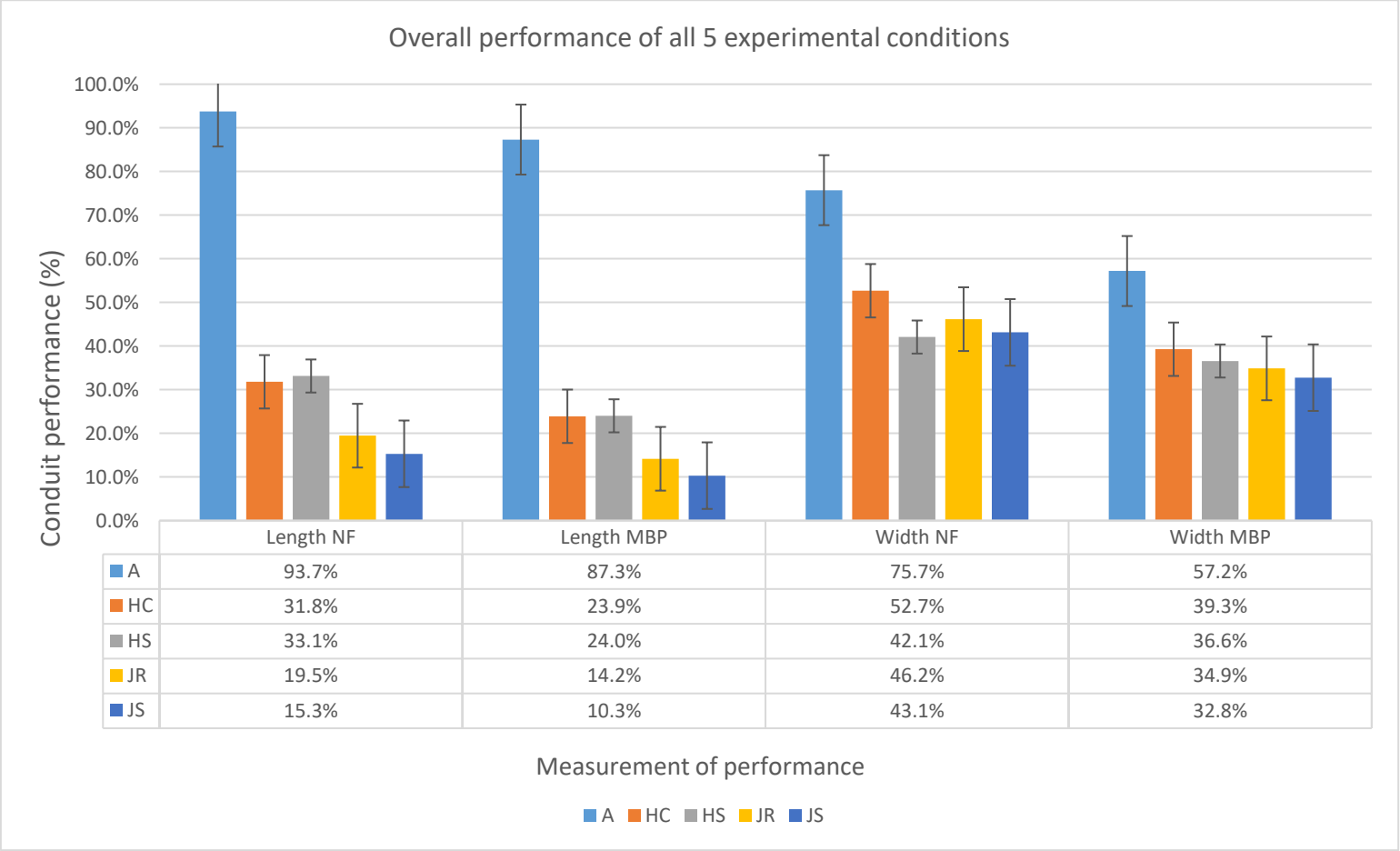

	Length NF	Length MBP	Width NF	Width MBP
A	93.7%	87.3%	75.7%	57.2%
HC	31.8%	23.9%	52.7%	39.3%
HS	33.1%	24.0%	42.1%	36.6%
JR	19.5%	14.2%	46.2%	34.9%
JS	15.3%	10.3%	43.1%	32.8%

Tableau 3. – Overall comparative performance of each experimental conduit condition. Measurements in mm and in %. NF= neurofilament, MBP= myelin basic protein. Experimental conditions: A= Autograft condition, HC= Hollow conduit without silk PEM, HS= Hollow conduit with silk PEM, JR= Jelly roll without silk PEM, JS= Jelly roll with silk PEM

4. Chapter 4 – Discussion

4.1 Discussion

Peripheral nerve injury resulting in physical gaps can be treated by grafting with the surgical gold standard, the autograft, and harnessing the peripheral nervous system's natural ability to regenerate albeit at a slow and complex way. However, use of the autograft has several flaws that may limit its use in clinical settings. As a result, attempts by different research teams have sought to develop alternative means to address peripheral nerve injury by creating nerve guidance conduits. Throughout the years, multiple biomaterials have been suggested along with increasing numbers of characteristics to include on the surface of the biomaterials or within the intraluminal space of the conduit, all in the effort to create a better performing conduit than the previous generations of nerve guidance conduits. In a study conducted by Landry et al. (Landry, 2017), silk PEM has shown to be able to support the growth of dorsal root ganglia *in vitro* when used as a substrate in cell culture. However, its abilities to support peripheral nerves have not been demonstrated in a *in vivo* situation. Therefore, we hypothesized that by coating conduits with silk PEM, we might observe enhanced peripheral nerve regeneration. Furthermore, in this study, we have proposed a novel conduit design called the "jelly roll", which consists of spreading fibrin glue onto a measured and pre-cut sheet of collagen and then rolling it onto itself, as an alternative conduit design to better support peripheral nerve regeneration than the hollow conduit design in a laceration and repair model using a rat animal model (Beaumont, 2009). We hypothesized that the layers of collagen that would settle inside the intraluminal space would provide additional contact guidance for regenerating axons, thus facilitating their regeneration throughout the nerve conduit (Jiang, 2010; Muheremu, 2015).

The length and width of regenerating axons in each experimental condition were measured to assess the robustness and volume of regeneration occurring. These measurements were then compared to the overall length and width of the conduits themselves to determine how much these regenerating axons have penetrated the conduit and how much space they occupy. To avoid artificially inflating the width measurements of regenerating axons, only the bundles of

fibers were taken into consideration and empty spaces between bundles were ignored as demonstrated in Figure 12. As for length measurements, only the furthest fibers extending from the proximal coaptation site without interruption were considered.

In order to visualize the stages of regeneration occurring inside the conduits, each specimen was stained by immunohistochemistry using neurofilament and MBP antibodies. Neurofilament highlights where regenerating fibers have grown inside the conduit while MBP determines how much of those fibers have been myelinated (Meller, 1993; Bodhireddy, 1994).

Preliminary results from the experiments in this study have shown that, after 4 weeks, conduits coated with silk PEM support peripheral nerve regeneration at a similar rate than their non-coated counterparts in the rat sciatic nerve. In addition, results have also shown that the novel jelly roll design did not promote axonal regeneration in a capacity that was superior to the classic design of the hollow conduit. Furthermore, of all the experimental conditions, the autograft remained the superior conduit for supporting peripheral nerve regeneration.

4.1.1 Performance of conduits coated with silk PEM

In this study, the hollow conduit with silk PEM condition demonstrated similar results as its non-silk counterpart. Indeed, when looking at their overall performance, in the silk-coated hollow conduit condition, 33.1% of neurofilament fibers have regenerated throughout the conduit compared to 31.8% in the non-silk coated hollow conduit condition. A similar pattern was observed for the MBP fibers in silk conduits where they reached 24.0% of the length of the conduit as opposed to 23.9% in hollow conduits without silk (Table 3). The hollow conduits slightly did better at supporting regenerating axons across their width than those with silk PEM (52.7% vs. 42.1% for neurofilament and 39.3% vs. 36.6% for MBP, respectively) (Table 3). When looking at axonal regeneration, neurofilament fibers were always found further down in the conduit and occupied a wider region at various locations within the conduit than MBP (Figure 14 and 15 and Table 2 and 3). This observation is consistent with previous studies as regenerating axons must first go through the process of a growth cone, followed by Schwann cell infiltration and neurotrophic factors secretion before they can extend from the site of injury first at the proximal

nerve stump. Only after 3 to 4 weeks post-injury can remyelination occur (Caillaud, Richard, Vallat, Desmoulière, & Billet, 2019).

When looking at individual hollow conduit performances, HS1 slightly performed better than the other conduits in supporting axonal regeneration throughout its length (49.5% for neurofilament and 38.7% for MBP) (Table 2). It should be noted that there were noticeable differences in the performance between the two hollow conduits with silk PEM (HS1 and HS2). HS1 has consistently outperformed HS2 in every single performance measurement in length and width for both neurofilament and MBP (Table 2). When we look at the appearance of each conduit, HS1 has a much straighter shape which allows the regenerating axons from the proximal end to enter the conduit from a more direct angle (Figure 14). In addition, the proximal end is better aligned with the opening of conduit than in HS2. When we observe the placement of the collagen walls in HS2, a noticeable narrowing to the beginning of the conduit can be seen. Moreover, the conduit's shape is curved in an "S" shape compared to HS1 which may cause the collagen walls to bend, thus resulting in twists and turns and dead ends which may slow down the rate of growth for regenerating axons that are seeking a way through. This is reflected in the performance of HS2 as regenerating axons only achieved 16.7% (neurofilament) and 9.1% (MBP) growth throughout the length of the conduit and width coverage has been less than 50% at the proximal site (Table 2). This would mean that despite entering a regenerative state after nerve trauma and despite a time point of 4 weeks, regenerating axons from the proximal nerve stump had great difficulty entering HS2.

A similar observation was made regarding the performance of the jelly roll with silk PEM condition in comparison to the jelly roll without silk PEM. JS1 performed relatively similarly to both jelly roll conduits without silk PEM (JR1 and JR2) in its ability to support neurofilament and MBP regeneration throughout the length of the conduit (Table 2). JS1 also performed better than JS2 in supporting regeneration lengthwise throughout the conduit (20.3% vs. 11.1% for neurofilament and 13.6% vs. 7.5% for MBP). Their width coverage percentage differed by only a few percent when measuring neurofilament width regeneration at the proximal end (59.4% vs. 64.3%) and their width coverage for MBP was the same (51.1%). However, by observation, the width of regenerating axons in JS2 narrowed greatly more than those found in JS1. The

inconsistencies between JS1 and JS2 may be due to the structural integrity of the openings of the conduit during implantation. It is possible that during surgical implantation, the intraluminal walls of collagen may have folded onto themselves, thus, restricting the opening of the proximal end (Figure 16). Overall, when considering the similarity in the performance of silk PEM-coated conduits in comparison to their non-silk PEM coated homologue conduits, it is possible that the narrow opening and the winding nature of a conduit could have caused regenerating axons to have an impeded access to the proximal end of the conduit and impaired regeneration through the conduit.

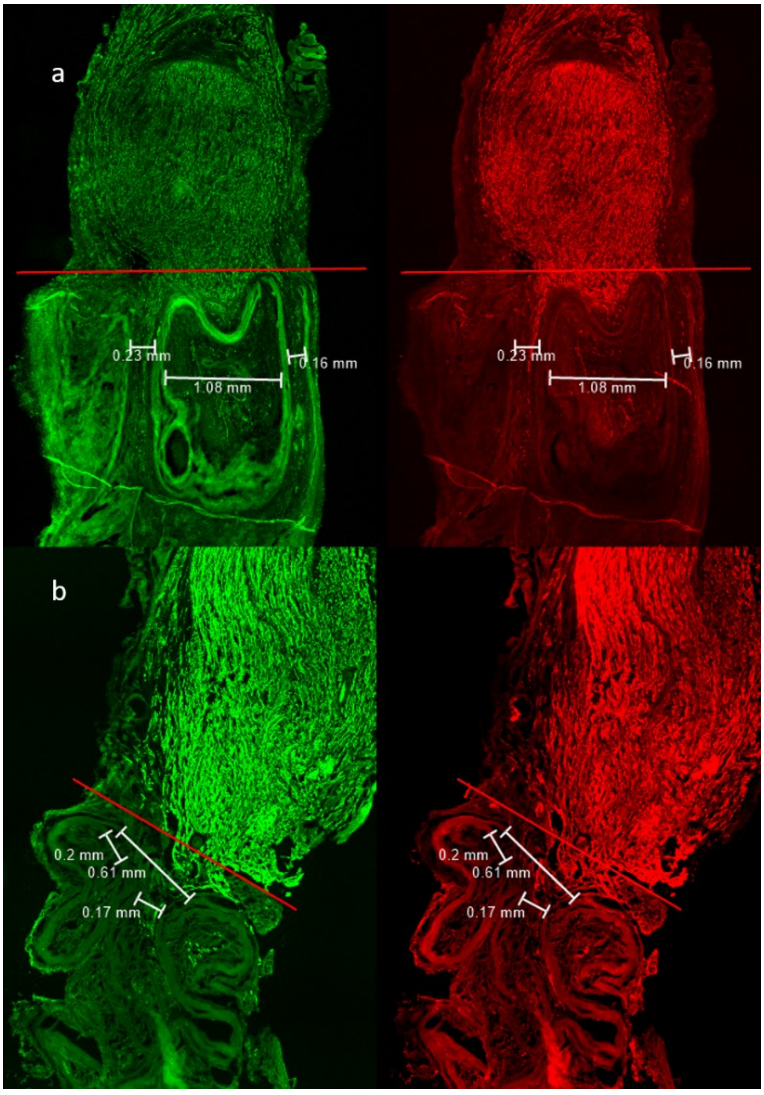

Figure 16. – Restricted axonal regeneration from the proximal end in the jelly roll conditions due to folds and bottlenecks caused by collagen walls. In this sample of JR1 (a) and JS2 (b), the

collagen walls form narrow corridors for regenerating axons from the proximal nerve stump, thus, forming a bottleneck (marked by measuring bars). However, it is important to keep in mind that these images only show one slice of sample out of many and therefore, these potential bottlenecks may widen in other sample slices of the conduit such as the 1.08mm area found in JR1 (a). Measurements in mm. a) Jelly roll without silk PEM 1 (JR1), b) Jelly roll with silk PEM 2 (JS2).

Due to the fact that very little difference was observed between the hollow conduits and jelly rolls conduits with and those without silk PEM, my *in vivo* studies did not show that silk PEM provides much improvement over non-coated collagen conduits. Despite limited sample size and other possible confounding factors that may have affected the performance of each individual conduit, the results of this study suggest that silk PEM does not perform better than collagen alone at supporting the regeneration of peripheral neurons. It is possible that support for axonal regeneration by silk PEM *in vitro* does not translate into the *in vivo* condition, or possibly that the advantageous feature of silk PEM in supporting hippocampal neuron outgrowth is not seen in peripheral neurons. Further studies should look deeper into its usage for peripheral nerve regeneration especially in *in vivo* situations.

4.1.2 Performance of the jelly roll design vs. the hollow conduit design

To evaluate the overall performance of our proposed novel conduit design (the jelly roll), we investigated the performance of both jelly roll conditions (with and without silk PEM) and compared them to the performance of both hollow conduit conditions (with and without silk PEM). After 4 weeks, we observed that the jelly roll with silk PEM and without silk PEM conditions failed to achieve similar performance than the hollow conduits with and without silk PEM conditions across all length performance metrics (Table 3). In fact, the hollow conduit conditions achieved 31.8% to 33.1% (HC and HS, respectively) for their length performance in neurofilament while the jelly roll designs achieved 19.5% and 15.3% (JR and JS, respectively) in neurofilament length performance (Table 3). When comparing MBP length performance, the hollow conduits also outperformed the jelly roll conduits (23.9% (HC) and 24.0% (HS) vs. 14.2% (JR) and 10.3% (JS))

On the other hand, both conduit designs achieved similar performance for the width covered by neurofilament and MBP at both the proximal end (Table 3).

These observations would suggest that the hollow conduit design allows further axonal penetration throughout the conduit's length after 4 weeks than the jelly roll design. In addition, these results also suggest that as regenerating fibers enter the conduit, they propagate throughout as much space as possible as long as they are not obstructed by physical barriers. This is further supported when looking at the intraluminal space inside the jelly roll (Figure 16). The collagen walls in the jelly roll conduit form narrow corridors allowing limited passage for regenerating axons coming from the proximal nerve stump, and therefore, may be causing a bottleneck at the proximal coaptation site which would restrict how much space is available for regenerating axons to access as they go further inside the conduit. As a result, instead of offering more contact guidance to axons, the intraluminal layers of collagen inside the jelly roll conduit may be more of a nuisance than otherwise. However, it is also possible that these bottlenecks only form at certain layers within the conduit and the narrow passages may widen throughout deeper layers of the conduit.

Furthermore, at the time of nerve harvest, thick scarring tissue was observed (Figure 17). It is a possibility that the scar tissue may have blocked nerve regeneration in the conditions where a conduit was implanted as compared to the autograft where less physical scarring was visible.

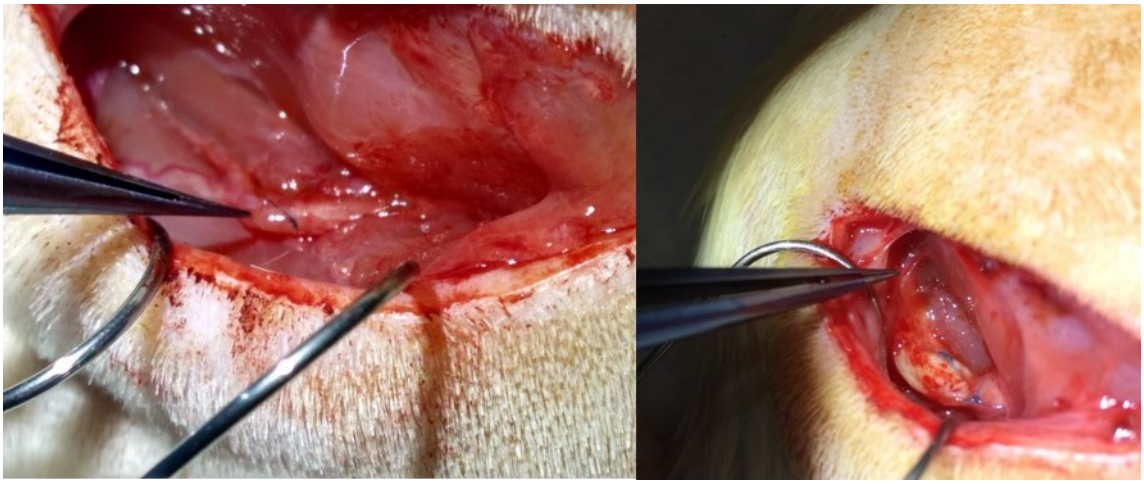

Figure 17. – Scar tissue formation around the sciatic nerve. Scarring tissue formation observed around the sciatic nerve at the time of harvest (4 weeks post-implantation).

In a previous study, Lemke et al. established a rat model to replicate post-surgical complications related to the formation of scar tissue (Lemke et al., 2017). The authors described that after 3 weeks, the rat sciatic nerve appeared to be swollen which by itself would indicate that intraneural or perineural fibrosis had occurred which was further confirmed by histopathological and electrophysiological verification. Indeed, during the harvest surgery which occurred 4 weeks after the implantation of the conduit, thick scar tissue was found enveloping every implanted conduit which may indicate that the implantation surgery caused a big enough trauma to cause serious scar tissue formation. In addition, in the case of scar tissue formation around the nerve conduit (extraneural), it can cause the nerve conduit to adhere to adjacent tissues which could deform the initially straight form of the conduit and the longitudinal sliding movement of the nerve (Hunter, 1991; Servet, Bekler, Kılınçoğlu, Özler, & Özkut, 2016). As such, adherence to adjacent tissue due to extraneural scar tissue formation may be a potential explanation for the deformation in the shape of the nerve conduits explained in the previous section. In future studies, scarring tissue interference with regeneration can be investigated through histological means.

4.1.3 Performance of the autograft compared to the other experimental conditions

Among all 5 experimental conditions, the autograft condition performed the best at supporting the furthest regenerating axons through the conduit and filling the widest space within the conduit at all locations (Table 3). The condition's overall performance outscored all other conditions in every metric as it supported 93.7% of neurofilament and 87.3% of MBP in length, and 75.7% and 57.2% of the width of the conduit was filled with neurofilament and MBP respectively. All other conditions had a performance level of under 50% in every performance measurement with the exception of the hollow conduit without silk PEM which achieved 52.7% of width coverage for neurofilament (Table 3). Furthermore, when looking at individual conduit performance, after 4 weeks, both autograft conduits supported over 90% of neurofilament length regeneration and over 80% of myelination while the next best performing conduit only reached 49.5% for neurofilament and 38.7% for MBP (Table 2).

These observations support the use of nerve autograft as the clinical gold standard for nerve repair. In a previous study conducted in 2019, a novel polyglycolic acid (PGA) conduit, containing collagen fiber within the tube was compared to a hollow collagen conduit and a nerve autograft (Saltzman et al., 2019). The authors found that the autograft condition outperformed the other two conditions both after 12 weeks and 16 weeks while the hollow conduit did better than the novel PGA conduit.

The superior performance of the nerve autograft condition may be explained by the nature of the nerve's intrinsic anatomy. The sciatic nerve contains fascicles that house motor and sensory fibers. Upon laceration, the anatomical structures are damaged, and their functions are also affected. To ensure the best restoration of nerve function, nerve fascicles from the proximal nerve stump must reconnect with fascicles with the same functional property (Xie et al., 2009; Zhong et al., 2015). As such if the fascicles cannot be matched and reconnected accurately with each other based on their functional property, the regenerating nerve fibers will not grow inside the proper channels, and sensory and motor functions will be lost (Zhong, 2015; Xie, 2009). The autograft possesses the advantage in that it is better suited to accommodate the appropriate neurotrophic factors and viable Schwann cells to aid axonal regeneration and nerve repair (Manoukian, 2019). To provide probable comparison between the autograft condition and experimental conduit conditions, future studies could investigate a decellularized nerve against experimental conditions or instead inject live SCs inside their experimental conditions.

In addition, it is possible that the fascicular structures have remained within the conduit which may have facilitated such rapid regeneration within the rat sciatic nerve while the other experimental conditions lacked any of the intraluminal architecture to support segregation of regenerating fibers according to their specific functional roles (sensory versus motor). Whether these regenerated fibers lead to appropriate motor and sensory recovery after 4 weeks remains to be determined with future studies.

4.2 Future research

Future studies should continue investigating the performance between silk-coated and non-silk coated conduits during a longer time period and with a higher sample size. Future studies should

also investigate further various intraluminal conduit designs in order to offer structures more like the innate architecture found inside peripheral nerves. In addition, Ankaferd Blood Stopper (ABS) solution may be used to prevent excessive epineural and extraneural scar tissue formation which may lead nerve conduits to adhere to adjacent tissues and thus, leading to the deformation of their shape (Servet et al., 2016).

Future studies could also utilise computer imaging techniques in order to generate additional metrics of conduit performance such as determining the density of nerve regeneration throughout a conduit. Imaging techniques utilised for MRI imaging can convert image pixels representing neurofilaments or MBP into a surface area of interest which can then be compared to the conduit's overall surface area.

4.3 Clinical implications

This study demonstrates that several factors must be considered regarding the performance of a nerve guidance conduit. The nature of the biomaterial is essential but other elements such as the shape of the conduit throughout its usage within the nerve is critical in order to avoid creating bottlenecks from the walls of the conduit which may limit the rate of axonal regeneration. Furthermore, the results obtained from this study may demonstrate that the intraluminal arrangement and architecture of a nerve conduit must resemble more closely the natural architecture of an intact nerve. We hope that these considerations may help future research attain a better performing nerve conduit that may, one day, match and outperform the autograft for peripheral nerve repair.

4.4 Study limitations

During this study, I encountered several limitations which prevented definitive conclusions regarding this study. Due to the SARS-CoV-2 outbreak, which causes COVID-19, that occurred at the end of 2019 and subsequently becoming a global pandemic by early 2020, the COVID-19 outbreak caused serious disruptions to my research activities. All research activities were suspended during the 2020 summer which caused the cancellation of a larger study involving a

total of 45 rats. This larger study would have seen the performance of the same five experimental conditions across 3 time points (4, 8 and 12 weeks) with 3 rats per group.

Furthermore, nerve conduit and tissue fixation by 4% PFA was established for 1h post-surgery for consistency between the experimental groups. However, it is possible that 1h of fixation by 4% PFA for the jelly roll conditions was not enough as upon being sectioned in the cryostat, the tissue in the sample was brittle, and was regularly shredded by the blade during the cutting motion. Furthermore, samples were cut from the distal end to the proximal end which often resulted in the shredding effect, however, when experimenting with the direction of cutting, I found that when cutting from the proximal end to the distal resulted in better tissue integrity. Additional problems which may have resulted from the time fixation by 4% PFA is that the layers of sample closer to the core may not have been fixed which would make it more difficult for the primary and secondary antibodies to bind during histochemistry. The lack of antibody binding to the proteins of interest would cause a lower fluorescent signal when observed under the microscope.

Finally, improper surgical attachment of the conduit to the nerve stumps may have been the cause behind some of the collapsed collagen walls observed at the proximal coaptation site which would have impeded axonal outgrowth into the conduit. Furthermore, the nature of the collagen sheet may have been inadequate as moisture would cause the collagen conduits to lose their structural integrity and thus, lose their shape. As a result, a more rigid form of collagen sheet should be used in future studies.

5. Chapter 5 – Conclusion

5.1 Conclusion

In conclusion, based on this pilot project, nerve grafts in the form of autografts remain the better surgical option to treat peripheral nerve injury. In addition, silk PEM was shown to support peripheral nerve regeneration in an *in vivo* setting during 4 weeks in an animal model. However, my results show that silk PEM based conduits performed similarly to their non-silk PEM based conduits and do not lead to higher performance in axonal regeneration along the length or the width of the conduit. Furthermore, the novel conduit design in the form of the jelly roll underperformed in comparison to the hollow conduit model. The fragile nature of the collagen in the jelly roll configuration lead to intraluminal layers of collagen to collapse, thus leading to impeded axonal regeneration into the proximal end of the conduit and leading the conduit to lose its overall shape which caused potential turns and dead ends which negatively impacted axonal outgrowth throughout the conduit. This study offers a good framework to evaluate the performance of nerve guidance conduits to support peripheral nerve regeneration through various metrics. This framework offers a comparative method to evaluate the performance of proposed conduit characteristics (inclusion of silk PEM coating) or proposed conduit designs (jelly roll) in respect to a baseline. Future studies may further elucidate whether silk PEM can definitively enhance peripheral nerve regeneration over non silk PEM based conduits which could lead to greater clinical significance and use.

Acknowledgements

I would like to thank Dr. Jenny Lin for her unconditional support and her guidance (both academic and professional) throughout the duration of my Master's. A big thank you to Michel Paquet, Vincent Cheung, Victoria Chang and Anaïs Robert for their technical assistance during the experiments. A thank you to Elke Kuster from the plateforme d'imagerie microscopique (PIM) and Ricardo Claudio from the animal care facility at CHU Sainte-Justine. I am also thankful to Dr. Timothy E. Kennedy for allowing me to use his lab at the Montreal Neurological Institute for the experiments and to Dr. Christopher J. Barrett for sharing his immense expertise on silk fibroin and its application in regenerative medicine. The research project was supported by the Institut TransMedTech (iTMT), le Fonds Apogée and the Faculté des études supérieures postdoctorales de l'Université de Montréal (FESP).

References

Andersen, C. R., Schmidt, A. H., Fitzgerald, C. B., Tintle, L. S., Helgeson, M. M., Lehman, L. R., . . . Ficke, C. J. (2015). Extremity War Injuries IX: Reducing Disability Within the Military. *J Am Acad Orthop Surg, 23*(8), e13-26. doi:10.5435/jaaos-d-15-00205

Beaumont, E., Cloutier, F. C., Atlan, M., Rouleau, D. M., & Beaumont, P. H. (2009). Chondroitinase ABC and acute electrical stimulation are beneficial for muscle reinnervation after sciatic nerve transection in rats. *Restor Neurol Neurosci, 27*(4), 297-305. doi:10.3233/rnn-2009-0479

Bittner, G. D., Schallert, T., & Peduzzi, J. D. (2000). Degeneration, Trophic Interactions, and Repair of Severed Axons: A Reconsideration of Some Common Assumptions. *6*(2), 88-109. doi:10.1177/107385840000600207

Bodhireddy, S. R., Lyman, W. D., Rashbaum, W. K., & Weidenheim, K. M. (1994). Immunohistochemical detection of myelin basic protein is a sensitive marker of myelination in second trimester human fetal spinal cord. *J Neuropathol Exp Neurol, 53*(2), 144-149. doi:10.1097/00005072-199403000-00005

Caillaud, M., Richard, L., Vallat, J. M., Desmoulière, A., & Billet, F. (2019). Peripheral nerve regeneration and intraneural revascularization. *Neural Regen Res, 14*(1), 24-33. doi:10.4103/1673-5374.243699

Chen, Z. L., Yu, W. M., & Strickland, S. (2007). Peripheral regeneration. *Annu Rev Neurosci, 30*, 209-233. doi:10.1146/annurev.neuro.30.051606.094337

Childe, J. R., Regal, S., Schimoler, P., Kharlamov, A., Miller, M. C., & Tang, P. (2018). Fibrin Glue Increases the Tensile Strength of Conduit-Assisted Primary Digital Nerve Repair. *Hand (N Y), 13*(1), 45-49. doi:10.1177/1558944717691131

Chiu, D. T., & Strauch, B. (1990). A prospective clinical evaluation of autogenous vein grafts used as a nerve conduit for distal sensory nerve defects of 3 cm or less. *Plast Reconstr Surg, 86*(5), 928-934. doi:10.1097/00006534-199011000-00015

Cho, M. S., Rinker, B. D., Weber, R. V., Chao, J. D., Ingari, J. V., Brooks, D., & Buncke, G. M. (2012). Functional outcome following nerve repair in the upper extremity using processed nerve allograft. *J Hand Surg Am, 37*(11), 2340-2349. doi:10.1016/j.jhsa.2012.08.028

Ciaramitaro, P., Mondelli, M., Logullo, F., Grimaldi, S., Battiston, B., Sard, A., . . . Cocito, D. (2010). Traumatic peripheral nerve injuries: epidemiological findings, neuropathic pain and quality of life in 158 patients. *J Peripher Nerv Syst, 15*(2), 120-127. doi:10.1111/j.1529-8027.2010.00260.x

de Ruiter, G. C., Malessy, M. J., Yaszemski, M. J., Windebank, A. J., & Spinner, R. J. (2009). Designing ideal conduits for peripheral nerve repair. *Neurosurg Focus, 26*(2), E5. doi:10.3171/FOC.2009.26.2.E5

Deumens, R., Bozkurt, A., Meek, M. F., Marcus, M. A., Joosten, E. A., Weis, J., & Brook, G. A. (2010). Repairing injured peripheral nerves: Bridging the gap. *Prog Neurobiol, 92*(3), 245-276. doi:10.1016/j.pneurobio.2010.10.002

Dubey, N., Letourneau, P. C., & Tranquillo, R. T. (2001). Neuronal contact guidance in magnetically aligned fibrin gels: effect of variation in gel mechano-structural properties. *Biomaterials, 22*(10), 1065-1075. doi:10.1016/s0142-9612(00)00341-0

Faroni, A., Mobasseri, S. A., Kingham, P. J., & Reid, A. J. (2015). Peripheral nerve regeneration: experimental strategies and future perspectives. *Adv Drug Deliv Rev, 82-83*, 160-167. doi:10.1016/j.addr.2014.11.010

FF, I., Nicolai, J. P., & Meek, M. F. (2006). Sural nerve donor-site morbidity: thirty-four years of follow-up. *Ann Plast Surg, 57*(4), 391-395. doi:10.1097/01.sap.0000221963.66229.b6

Gerth, D. J., Tashiro, J., & Thaller, S. R. (2015). Clinical outcomes for Conduits and Scaffolds in peripheral nerve repair. *World J Clin Cases, 3*(2), 141-147. doi:10.12998/wjcc.v3.i2.141

Griffin, J. W., Hogan, M. V., Chhabra, A. B., & Deal, D. N. (2013). Peripheral nerve repair and reconstruction. *J Bone Joint Surg Am, 95*(23), 2144-2151. doi:10.2106/JBJS.L.00704

Grinsell, D., & Keating, C. P. (2014). Peripheral nerve reconstruction after injury: a review of clinical and experimental therapies. *Biomed Res Int, 2014*, 698256. doi:10.1155/2014/698256

Hadlock, T., Sundback, C., Hunter, D., Cheney, M., & Vacanti, J. P. (2000). A polymer foam conduit seeded with Schwann cells promotes guided peripheral nerve regeneration. *Tissue Eng, 6*(2), 119-127. doi:10.1089/107632700320748

Hallgren, A., Björkman, A., Chemnitz, A., & Dahlin, L. B. (2013). Subjective outcome related to donor site morbidity after sural nerve graft harvesting: a survey in 41 patients. *BMC Surg, 13*, 39. doi:10.1186/1471-2482-13-39

Hoben, G. M., Ee, X., Schellhardt, L., Yan, Y., Hunter, D. A., Moore, A. M., . . . Wood, M. D. (2018). Increasing Nerve Autograft Length Increases Senescence and Reduces Regeneration. *Plast Reconstr Surg, 142*(4), 952-961. doi:10.1097/PRS.0000000000004759

Hunter, J. M. (1991). Recurrent carpal tunnel syndrome, epineural fibrous fixation, and traction neuropathy. *Hand Clin, 7*(3), 491-504.

Jackson, M. R. (2001). Fibrin sealants in surgical practice: An overview. *Am J Surg, 182*(2 Suppl), 1s-7s. doi:10.1016/s0002-9610(01)00770-x

Jiang, X., Lim, S. H., Mao, H. Q., & Chew, S. Y. (2010). Current applications and future perspectives of artificial nerve conduits. *Exp Neurol, 223*(1), 86-101. doi:10.1016/j.expneurol.2009.09.009

Karabekmez, F. E., Duymaz, A., & Moran, S. L. (2009). Early clinical outcomes with the use of decellularized nerve allograft for repair of sensory defects within the hand. *Hand (N Y), 4*(3), 245-249. doi:10.1007/s11552-009-9195-6

Konofaos, P., & Ver Halen, J. P. (2013). Nerve repair by means of tubulization: past, present, future. *J Reconstr Microsurg, 29*(3), 149-164. doi:10.1055/s-0032-1333316

Kouyoumdjian, J. A. (2006). Peripheral nerve injuries: a retrospective survey of 456 cases. *Muscle Nerve, 34*(6), 785-788. doi:10.1002/mus.20624

Landry, M. J., Gu, K., Harris, S. N., Al-Alwan, L., Gutsin, L., De Biasio, D., . . . Barrett, C. J. (2019). Tunable Engineered Extracellular Matrix Materials: Polyelectrolyte Multilayers Promote Improved Neural Cell Growth and Survival. *Macromol Biosci, 19*(5), e1900036. doi:10.1002/mabi.201900036

Langer, S., Schildhauer, T., Dudda, M., Sauber, J., & Spindler, N. (2015). Fibrin glue as a protective tool for microanastomoses in limb reconstructive surgery.

Lemke, A., Penzenstadler, C., Ferguson, J., Lidinsky, D., Hopf, R., Bradl, M., . . . Hausner, T. (2017). A novel experimental rat model of peripheral nerve scarring that reliably mimics post-surgical complications and recurring adhesions. *Dis Model Mech, 10*(8), 1015-1025. doi:10.1242/dmm.028852

Li, Y., Meng, H., Liu, Y., & Lee, B. P. (2015). Fibrin gel as an injectable biodegradable scaffold and cell carrier for tissue engineering. *ScientificWorldJournal, 2015*, 685690. doi:10.1155/2015/685690

Lietz, M., Dreesmann, L., Hoss, M., Oberhoffner, S., & Schlosshauer, B. (2006). Neuro tissue engineering of glial nerve guides and the impact of different cell types. *Biomaterials, 27*(8), 1425-1436. doi:10.1016/j.biomaterials.2005.08.007

Magaz, A., Faroni, A., Gough, J. E., Reid, A. J., Li, X., & Blaker, J. J. (2018). Bioactive Silk-Based Nerve Guidance Conduits for Augmenting Peripheral Nerve Repair. *Adv Healthc Mater, 7*(23), e1800308. doi:10.1002/adhm.201800308

Manoukian, O. (2019). Biopolymer-Nanotube Nerve Guidance Conduit Drug Delivery for Peripheral Nerve Regeneration.

Marchesi, C., Pluderi, M., Colleoni, F., Belicchi, M., Meregalli, M., Farini, A., . . . Torrente, Y. (2007). Skin-derived stem cells transplanted into resorbable guides provide functional nerve regeneration after sciatic nerve resection. *Glia, 55*(4), 425-438. doi:10.1002/glia.20470

Martins, R. S., Barbosa, R. A., Siqueira, M. G., Soares, M. S., Heise, C. O., Foroni, L., & Teixeira, M. J. (2012). Morbidity following sural nerve harvesting: a prospective study. *Clin Neurol Neurosurg, 114*(8), 1149-1152. doi:10.1016/j.clineuro.2012.02.045

Meller, D., Bellander, B. M., Schmidt-Kastner, R., & Ingvar, M. (1993). Immunohistochemical studies with antibodies to neurofilament proteins on axonal damage in experimental focal lesions in rat. *J Neurol Sci, 117*(1-2), 164-174. doi:10.1016/0022-510x(93)90169-y

Menorca, R. M., Fussell, T. S., & Elfar, J. C. (2013). Nerve physiology: mechanisms of injury and recovery. *Hand Clin, 29*(3), 317-330. doi:10.1016/j.hcl.2013.04.002

Moore, A. M., Ray, W. Z., Chenard, K. E., Tung, T., & Mackinnon, S. E. (2009). Nerve allotransplantation as it pertains to composite tissue transplantation. *Hand (N Y), 4*(3), 239-244. doi:10.1007/s11552-009-9183-x

Muheremu, A., & Ao, Q. (2015). Past, Present, and Future of Nerve Conduits in the Treatment of Peripheral Nerve Injury. *Biomed Res Int, 2015*, 237507. doi:10.1155/2015/237507

Noble, J., Munro, C. A., Prasad, V. S., & Midha, R. (1998). Analysis of upper and lower extremity peripheral nerve injuries in a population of patients with multiple injuries. *J Trauma, 45*(1), 116-122. doi:10.1097/00005373-199807000-00025

Pabari, A., Lloyd-Hughes, H., Seifalian, A. M., & Mosahebi, A. (2014). Nerve conduits for peripheral nerve surgery. *Plast Reconstr Surg, 133*(6), 1420-1430. doi:10.1097/prs.0000000000000226

Pfister, B. J., Gordon, T., Loverde, J. R., Kochar, A. S., Mackinnon, S. E., & Cullen, D. K. (2011). Biomedical engineering strategies for peripheral nerve repair: surgical applications, state of the art, and future challenges. *Crit Rev Biomed Eng, 39*(2), 81-124. doi:10.1615/critrevbiomedeng.v39.i2.20

Poppler, L. H., Parikh, R. P., Bichanich, M. J., Rebehn, K., Bettlach, C. R., Mackinnon, S. E., & Moore, A. M. (2018). Surgical interventions for the treatment of painful neuroma: a comparative meta-analysis. *Pain, 159*(2), 214-223. doi:10.1097/j.pain.0000000000001101

Pulley, B. R., Luo, T. D., Barnwell, J. C., Smith, B. P., Smith, T. L., & Li, Z. (2016). A chronically-denervated versus a freshly-harvested autograft for nerve repair in rats. *Hand Microsurg, 5*(3), 124-129. doi:10.5455/handmicrosurg.215015

Raichle, K. A., Hanley, M. A., Molton, I., Kadel, N. J., Campbell, K., Phelps, E., Ehde, D., & Smith, D. G. . (2008). Prosthesis use in persons with lower and upper-limb amputation. *Journal of rehabilitation research and development, 45*(7), 961–972. doi:https://doi.org/10.1682/jrrd.2007.09.0151

Riccio, M., Marchesini, A., Pugliese, P., & De Francesco, F. (2019). Nerve repair and regeneration: Biological tubulization limits and future perspectives. *J Cell Physiol, 234*(4), 3362-3375. doi:10.1002/jcp.27299

Rivera, J. C., Glebus, G. P., & Cho, M. S. (2014). Disability following combat-sustained nerve injury of the upper limb. *Bone Joint J, 96-b*(2), 254-258. doi:10.1302/0301-620x.96b2.31798

Sailer, M., Lai Wing Sun, K., Mermut, O., Kennedy, T. E., & Barrett, C. J. (2012). High-throughput cellular screening of engineered ECM based on combinatorial polyelectrolyte multilayer films. *Biomaterials, 33*(24), 5841-5847. doi:10.1016/j.biomaterials.2012.05.001

Saltzman, E. B., Villa, J. C., Doty, S. B., Feinberg, J. H., Lee, S. K., & Wolfe, S. W. (2019). A Comparison Between Two Collagen Nerve Conduits and Nerve Autograft: A Rat Model of Motor Nerve Regeneration. *J Hand Surg Am, 44*(8), 700.e701-700.e709. doi:10.1016/j.jhsa.2018.10.008

Schlosshauer, B., Dreesmann, L., Schaller, H. E., & Sinis, N. (2006). Synthetic nerve guide implants in humans: a comprehensive survey. *Neurosurgery, 59*(4), 740-747; discussion 747-748. doi:10.1227/01.NEU.0000235197.36789.42

Servet, E., Bekler, H., Kılınçoğlu, V., Özler, T., & Özkut, A. (2016). Effect of bleeding on nerve regeneration and epineural scar formation in rat sciatic nerves: an experimental study. *Acta Orthop Traumatol Turc, 50*(2), 234-241. doi:10.3944/aott.2015.15.0090

Siemionow, M., & Brzezicki, G. (2009). Chapter 8: Current techniques and concepts in peripheral nerve repair. *Int Rev Neurobiol, 87*, 141-172. doi:10.1016/s0074-7742(09)87008-6

Spinner, R. J., Shin, A. Y., & Bishop, A. T. (2015). Advances in the Repair of Peripheral Nerve Injury. *Neurosurgery, 62 Suppl 1*, 146-151. doi:10.1227/neu.0000000000000814

Swett, J. E., Wikholm, R. P., Blanks, R. H., Swett, A. L., & Conley, L. C. (1986). Motoneurons of the rat sciatic nerve. *Exp Neurol, 93*(1), 227-252. doi:10.1016/0014-4886(86)90161-5

Taylor, C. A., Braza, D., Rice, J. B., & Dillingham, T. (2008). The incidence of peripheral nerve injury in extremity trauma. *Am J Phys Med Rehabil, 87*(5), 381-385. doi:10.1097/PHM.0b013e31815e6370

Vollrath, F., Barth, P., Basedow, A., Engström, W., & List, H. (2002). Local tolerance to spider silks and protein polymers in vivo. *In Vivo, 16*(4), 229-234.

Wolvetang, N. H. A., Lans, J., Verhiel, S., Notermans, B. J. W., Chen, N. C., & Eberlin, K. R. (2019). Surgery for Symptomatic Neuroma: Anatomic Distribution and Predictors of Secondary Surgery. *Plast Reconstr Surg, 143*(6), 1762-1771. doi:10.1097/prs.0000000000005664

Xie, S., Xiang, B., Bu, S., Cao, X., Ye, Y., Lu, J., & Deng, H. (2009). Rapid identification of anterior and posterior root of cauda equina nerves by near-infrared diffuse reflectance spectroscopy. *14 %J Journal of Biomedical Optics*(2), 024005.

Yang, Y., Chen, X., Ding, F., Zhang, P., Liu, J., & Gu, X. (2007). Biocompatibility evaluation of silk fibroin with peripheral nerve tissues and cells in vitro. *Biomaterials, 28*(9), 1643-1652. doi:10.1016/j.biomaterials.2006.12.004

Yoshii, S., & Oka, M. (2001). Collagen filaments as a scaffold for nerve regeneration. *J Biomed Mater Res, 56*(3), 400-405. doi:10.1002/1097-4636(20010905)56:3<400::aid-jbm1109>3.0.co;2-7

Zhong, Y., Wang, L., Dong, J., Zhang, Y., Luo, P., Qi, J., . . . Xian, C. J. (2015). Three-dimensional Reconstruction of Peripheral Nerve Internal Fascicular Groups. *Sci Rep, 5*, 17168. doi:10.1038/srep17168